

Strong decay widths and mass spectra of charmed baryons

H. García-Tecocoatzi

*Department of Physics, University of La Plata (UNLP),
49 y 115 cc. 67, 1900 La Plata, Argentina and*

Center of High Energy Physics, Kyungpook National University, 80 Daehak-ro, Daegu 41566, Korea

A. Giachino

INFN, Sezione di Genova, Via Dodecaneso 33, 16146 Genova, Italy and

Institute of Nuclear Physics Polish Academy of Sciences Radzikowskiego 152, 31-342 Cracow, Poland

J. Li and A. Ramirez-Morales

Center of High Energy Physics, Kyungpook National University, 80 Daehak-ro, Daegu 41566, Korea

E. Santopinto*

INFN, Sezione di Genova, Via Dodecaneso 33, 16146 Genova, Italy

The total decay widths of the charmed baryons, including all the possible open-flavor decay channels, are calculated by means of the 3P_0 model. Our calculations consider in the final states: the charmed baryon-(vector/pseudoscalar) meson pairs and the (octet/decuplet) baryon-(pseudoscalar/vector) charmed meson pairs, within a constituent quark model. Furthermore, we calculate the masses of the charmed baryon ground states and their excitations up to the D -wave states. We also calculate the charmed baryon masses in a constituent quark model, both in the three-quark and in quark-diquark schemes, utilizing a Hamiltonian model based on a harmonic oscillator potential plus a mass splitting term that encodes the spin, spin-orbit, isospin, and flavor interactions. The parameters of the Hamiltonian model are fitted to experimental data of charmed baryon masses and decay widths. As the experimental uncertainties of the data affect the fitted model parameters, we have thoroughly propagated these uncertainties into our predicted charmed baryon masses and decay widths via a Monte Carlo bootstrap approach, which is often absent in other theoretical studies on this subject. Our quantum number assignments and predictions of mass and strong partial decay widths are in reasonable agreement with the available data. Thus, our results show the ability to guide future measurements in LHCb, Belle and Belle II experiments. Finally, the appendixes provide some details of our calculations, in which we include the flavor coupling coefficients, which are useful for further theoretical investigations into charmed baryon strong decay widths.

I. INTRODUCTION

The discovery of new baryon resonances in high-energy physics experiments always enriches our knowledge of the hadron zoo, and provides essential information to explain the fundamental forces that govern nature. In particular, the hadron mass patterns carry information regarding the way the quarks interact with one another, and provide further insight into the fundamental binding mechanism of matter at an elementary level.

The number of observed charmed baryons has increased owing to the LHCb and Belle experiments. In 2017, the LHCb collaboration announced the observation of five narrow Ω_c states in the $\Xi_c^+ K^-$ decay channel [1]. Later, Belle observed five resonant states in the $\Xi_c^+ K^-$ invariant mass distribution and unambiguously confirmed four of the states announced by LHCb, $\Omega_c(3000)$, $\Omega_c(3050)$, $\Omega_c(3066)$ and $\Omega_c(3090)$, although no signal was found for the $\Omega_c(3119)$ [2]. Belle also mea-

sured a signal excess at 3188 MeV, corresponding to the $\Omega_c(3188)$ state reported by LHCb [2]. In 2020, the LHCb collaboration observed three $\Xi_c^0(2923)$, $\Xi_c^0(2939)$ and $\Xi_c^0(2965)$ states [3]; however, the J^P quantum numbers were not reported. These results reported by LHCb implied that the broad state $\Xi_c^0(2930)$ observed by Belle [4] and BaBar [5] resolves into two narrower states $\Xi_c^0(2923)$ and $\Xi_c^0(2939)$. Nevertheless, a puzzle emerges in the experimental data, since Ref. [3] reported a narrow state with a central mass of about 2965 MeV, which is close to a resonance seen by the Belle collaboration at 2970 MeV [6, 7], and confirmed by the BaBar collaboration [8]; hence, further studies are required in order to determine whether these observations correspond to different baryons or to the same one. Moreover, the available charm baryon data are limited, especially for the Σ_c resonances; indeed, only three states reported are by the PDG [9], $\Sigma_c(2455)$, $\Sigma_c(2520)$ and $\Sigma_c(2800)$, while new analyses are being carried out in this sector [10]. More recently in 2021, the Belle collaboration measured the spin and parity of the $\Xi_c(2970)$ state to be $J^P = 1/2^+$ [11], under an assumption that the lowest partial wave dominates the decay.

*elena.santopinto@ge.infn.it

With regard to theory, the application of the non-relativistic quark model to the light baryon spectrum owes its origins to the pioneering investigations by Isgur and Karl [12, 13], which were further extended in [14] to the Λ_c and Σ_c baryons and to the Λ_b and Σ_b baryons in [15]. Over the last few years, interest in heavy-light baryon spectroscopy has grown once more. Examples of the recent ample literature on theoretical investigations into heavy baryon spectroscopy are: the report of the QCD-motivated relativistic quark-diquark model based on the quasi-potential approach [16, 17], the non-relativistic quark model [14, 18–20], and the QCD sum rules in the framework of the heavy quark effective theory (HQET) [21–24]. Alternative discussions employing other models can be found in Ref.[25–29], and lattice QCD studies in Ref. [30–33]. For extra references see the review articles [34–38]. Nevertheless, no model is capable of describing the complete baryon spectrum. Indeed, only few data determine the quantum numbers for the charm-baryon states; some of these kinds of assignments, are yet unmeasured, have been extracted from quark model predictions from the PDG [9]. Furthermore, it is unclear whether the heavy baryons behave as quark-diquark or three-quark systems. Thus, a full understanding of the internal structure of the charmed baryons still requires thorough theoretical and experimental studies.

Numerous studies have been conducted on the heavy baryon decay widths. Nevertheless, a complete calculation of all charm-baryon partial strong decay widths for ground and excited states up to the D -wave shell within the same model has never been performed. For example, within the framework of the chiral quark models in Ref. [39], only the open-flavor strong decay widths $\Lambda_c \rightarrow \Sigma_c \pi, D^0 p$ and $\Sigma_c \rightarrow \Lambda_c \pi, \Sigma_c \pi, D^0 p$ were calculated. Additionally, in Ref. [40] the Ξ'_c strong decays were considered up to the D -wave shell, while no predictions of the other charmed baryon decays were made. In Ref. [41] the authors calculated the S - and P -wave decay widths heavy baryons; however, their analysis was limited to baryons decaying only into ground-state charmed baryons plus pseudoscalar mesons. Moreover, no D -wave or radial excitations were reported. In the framework of the heavy hadron chiral perturbation theory in Ref. [42], certain decays of charmed baryons Λ_c, Σ_c and Ξ'_c baryons were computed although these calculations did not include the charmed baryon-vector meson channels and did not give predictions for the Ω_c states. In Ref. [43] the calculations were performed only for the S - and P -wave Λ_c, Σ_c and Ξ'_c states that decay into a ground-state charmed baryon plus a pion. Adopting a non-relativistic quark model, Ref. [44] evaluated only the decay widths of the charmed baryons $\Lambda_c^*(2595), \Lambda_c^*(2625), \Lambda_c^*(2765), \Lambda_c^*(2880)$ and $\Lambda_c^*(2940)$ into $\Sigma_c(2455)\pi$ and $\Sigma_c^*(2520)\pi$, and of $\Sigma_c(2455)$ and $\Sigma_c^*(2520)$ into $\Lambda_c \pi$, were evaluated. In a more recent work [45], the same decay widths were calculated by adding relativistic corrections, and the previous analysis was extended to the decay widths of bottom baryons. In the context of the elementary emission

model [46], the strong and radiative decays of charmed and bottom baryons were investigated. However, the study was restricted to the low-lying λ -mode D -wave excitations and the charmed baryon-vector meson channels or the charmed meson-octet/decuplet baryon channels were not included. In the framework of QCD sum rules in Ref. [47], the author studied only the P -wave $\Lambda_c \rightarrow \Sigma_c + \pi$ decays and the P -wave Λ_c electromagnetic decays, while in [48] the authors calculated the P -wave charmed baryon decays into ground-state charmed baryons accompanied by a pseudoscalar meson. In [49], the 3P_0 model was applied to calculate the strong decays of Λ_c, Σ_c , and Ξ_c excited states up to the D -wave shell. Nevertheless the decay widths into charmed baryon-vector mesons were not calculated, nor was the Ω_c sector considered. The 3P_0 model was also applied in [50–52]. In these references, however only the Λ_c decays were studied. In [20], the Eichten, Hill and Quigg formula, in combination with the 3P_0 model, was applied in order to calculate the $1P$ and $2S$ Λ_c, Σ_c and Ξ_c decays into charmed baryon and pseudoscalar mesons.

In Ref. [53], prompted by the observation of the five Ω_c by LHCb [1], we calculated the Ω_c decay widths in the $\Xi_c^+ K^-$ and $\Xi_c^0 K^-$ channels within the 3P_0 model. In that study, we also calculated the Ω_b decay widths in the $\Xi_b^+ K^-$ and $\Xi_b^0 K^-$ channels and gave predictions for the mass spectra of both Ω_c and Ω_b ground states and P -wave excitations. Subsequently, in Ref. [54], we extended our model to the Ξ'_c and the Ξ'_b states and calculated the mass spectra and the strong partial decay widths of the Ξ'_c -ground states and $-P$ -wave excitations into ${}^2\Sigma_c \bar{K}, {}^2\Xi'_c \pi, {}^2\Sigma_c \bar{K}, {}^4\Xi'_c \pi, \Lambda'_c \bar{K}, \Xi_c \pi$ and $\Xi_c \eta$ and of the Ξ'_b -ground states and $-P$ -wave excitations into ${}^2\Sigma_b \bar{K}, {}^2\Xi'_b \pi, {}^2\Sigma_b \bar{K}, {}^4\Xi'_b \pi, \Lambda'_b \bar{K}, \Xi_b \pi$ and $\Xi_b \eta$, within both the Elementary Emission Model (EEM) and the 3P_0 model. In the present article we further extend our model to the whole charm-baryon states (cqq, cqs and css systems) by employing the same mass formula originally introduced in Ref. [53]. Additionally, in the present paper, the parameters of the model are fitted in order to globally reproduce all the available charm-baryon experimental states. The experimental uncertainties are also propagated to the model parameters by means of the Monte Carlo bootstrap method [55], which is an advanced method used to properly estimate the error propagation by taking into account the correlation between the fitted parameters. In this way, we perform a global fit of a single model, in which the same set of parameters predicts the charm-baryon masses and strong partial decay widths in all the possible open decay channels up to the D -wave shell. Moreover, considering the well-established observation by Isgur and Karl in Ref. [12] that the harmonic oscillator wave functions are a good approximation of the eigenfunctions of low-lying states, and also taking into account that the calculations of the strong decay widths are barely sensitive to the specific model used [56], our strong partial decay width predictions are the most complete

calculations in the charm-baryon sector to date. The paper is organized as follows: In Sec. II, we introduce the details of the methodology used to construct the charm-baryon states and to calculate the mass spectra and decay widths. The theoretical details for the calculation of the charm-baryon mass spectra include contributions due to spin-orbit-, spin-, isospin- and flavor-dependent interactions. Thus, we develop a formalism for obtaining the S -, P - and D -wave charm-baryon mass spectrum. We also describe the calculation of the total-decay-width of the charmed baryons via the 3P_0 model by computing the partial-decay-width of all the open-flavor channels. In Sec. III, we carefully study the parameters of the mass formula presented in Ref. [53] and perform a global fit to the data on well-established charmed baryons and their uncertainties, as propagated by means of the bootstrap method. In Sec. IV, we present the masses and widths of all charmed baryons up to D -wave and discuss our assignments of all the available experimental data. In section V, we discuss our results within some limits and, finally, we calculate the mass splitting between the ρ - and λ -mode excitations of the charmed baryon resonances. This calculation is fundamental in order to access the inner heavy-light baryon structure, as the presence or absence of ρ -mode excitations in the experimental spectrum will be the key to distinguishing between the quark-diquark and three-quark behaviours. Finally, in Sec. VI, we state our conclusions.

II. METHODOLOGY

A. Mass spectra of charmed baryons

The masses of the charm-baryon states are calculated as the eigenvalues of the Hamiltonian system. The charm-baryon states are described in accordance with the formalism of Ref.[53], *i.e.*, the charm-baryon system is modeled with a three-dimensional harmonic oscillator (h.o.) Hamiltonian, $H_{\text{h.o.}}$, plus a perturbation operator that describes the spin, spin-orbit, isospin and flavor dependences of the mass splittings:

$$H = H_{\text{h.o.}} + P_s \mathbf{S}^2 + P_{sl} \mathbf{S} \cdot \mathbf{L} + P_I \mathbf{I}^2 + P_f \mathbf{C}_2(\text{SU}(3)_f), \quad (1)$$

\mathbf{S} , \mathbf{L} , \mathbf{I} and $\mathbf{C}_2(\text{SU}(3)_f)$ are the spin, orbital momentum, isospin and Casimir operators, respectively. This perturbation term contributes to the charm-baryon mass by adding the usual \mathbf{S} , \mathbf{L} , \mathbf{I} and $\mathbf{C}_2(\text{SU}(3)_f)$ eigenvalues weighted with the model parameters P_s , P_{sl} , P_I and P_f , as indicated in Eq. 1. Notice that our mass formula in Eq. 1 is independent of I_z , the isospin projection; therefore, the charge channels are degenerated in this model.

For the case in which the baryon is modeled as a three-quark system, the three-dimensional h.o. Hamiltonian

reads as,

$$H_{\text{h.o.}} = \sum_{i=1}^3 m_i + \frac{\mathbf{p}_\rho^2}{2m_\rho} + \frac{\mathbf{p}_\lambda^2}{2m_\lambda} + \frac{1}{2} m_\rho \omega_\rho^2 \rho^2 + \frac{1}{2} m_\lambda \omega_\lambda^2 \lambda^2 \quad (2)$$

written in terms of Jacobi coordinates, $\boldsymbol{\rho}$ and $\boldsymbol{\lambda}$, and conjugated momenta, \mathbf{p}_ρ and \mathbf{p}_λ . The $H_{\text{h.o}}$ eigenvalues are

$$\sum_{i=1}^3 m_i + \omega_\rho n_\rho + \omega_\lambda n_\lambda; \text{ with } \omega_{\rho(\lambda)} = \sqrt{\frac{3K_c}{m_{\rho(\lambda)}}}, \quad (3)$$

where m_i are the constituent quark masses, m_1 and m_2 correspond to the light quarks and m_3 to the charm quark; m_ρ is defined as $m_\rho = (m_1 + m_2)/2$, and $m_\lambda = 3m_\rho m_3 / (2m_\rho + m_3)$. We use the well-known definitions for $n_{\rho(\lambda)} = 2k_{\rho(\lambda)} + l_{\rho(\lambda)}$, $k_{\rho(\lambda)} = 0, 1, \dots$, and $l_{\rho(\lambda)} = 0, 1, \dots$; here, $l_{\rho(\lambda)}$ are the orbital angular momenta of the $\rho(\lambda)$ oscillators, and $k_{\rho(\lambda)}$ is the number of nodes (radial excitations) in the $\rho(\lambda)$ oscillators. K_c is the spring constant.

Additionally, we present a simplification of the three-quark system that utilizes only one relative coordinate \mathbf{r} and momentum \mathbf{p}_r , namely, the quark-diquark system. Here, the two light quarks are regarded as a single diquark object. The quark-diquark Hamiltonian reads as,

$$H_{\text{h.o.}} = m_D + m_c + \frac{\mathbf{p}_r^2}{2\mu} + \frac{1}{2} \mu \omega_r^2 r^2, \quad (4)$$

with $\mathbf{p}_r = (m_c \mathbf{p}_D - m_D \mathbf{p}_c) / (m_c + m_D)$. The $H_{\text{h.o}}$ eigenvalues are

$$m_D + m_c + \omega_r n_r; \text{ with } \omega_r = \sqrt{\frac{3K_c}{\mu}}, \quad (5)$$

where m_D is the diquark mass, m_c is the charm quark mass; μ is the reduced mass of the system, and is defined as $\mu = m_c m_D / (m_c + m_D)$; n_r and K_c are defined as in the three-quark system.

B. Charm-baryon states

In the three-quark model, the baryon states are characterized by means of a qqQ system, where $Q = c$ and $q = u, d, s$. The three-quark Hamiltonian in Eq.2 is expressed in terms of two coordinates, $\boldsymbol{\rho}$ and $\boldsymbol{\lambda}$ [57], that encode the spatial degrees of freedom of the system with associated effective masses, m_ρ and m_λ . Note that in heavy-light baryons, for which $m_\rho \ll m_\lambda$, the two excitation modes can be decoupled from each other as long as the heavy-light quark mass difference is significant.

In the quark-diquark system, the baryon states are characterized by means of a DQ system, where $Q = c$ and $D = D_\Omega, D_\Xi, D_{\Sigma, \Lambda}$ are the diquarks that correspond to the $\Omega_c, \Xi'_c(\Xi_c), \Sigma_c$ and Λ_c baryons, respectively. The

quark-diquark Hamiltonian in Eq.4 is expressed in terms of one spatial coordinate \mathbf{r} with an associated reduced mass μ ; *i.e.*, the quark-diquark system resembles a diatomic molecule.

We construct the ground and excited states in order to establish the quantum numbers of the charm-baryon states. We consider that a single quark is described by its spin, flavor, color and spatial degrees of freedom. Moreover, in our models, the light quarks behave as identical particles; hence, we take into account the Pauli principle, which postulates that the wave function of identical fermions must be anti-symmetric in order to achieve particle exchange. Thus, the qq spin-flavor and orbital wave functions have the same permutation symmetry: symmetric spin-flavor in the S -wave or D -wave, or anti-symmetric spin-flavor in the anti-symmetric P -wave. Two light quarks are necessary in the $\mathbf{6}_f$ or anti- $\mathbf{3}_f$ flavor-symmetric state.

Formally, a three-quark (quark-diquark) quantum state, written as $|l_\lambda(l_r), l_\rho, k_\lambda(k_r), k_\rho\rangle$, is defined by its total angular momentum $\mathbf{J}_{\text{tot}} = \mathbf{L}_{\text{tot}} + \mathbf{S}_{\text{tot}}$, where $\mathbf{L}_{\text{tot}} = \mathbf{l}_\rho + \mathbf{l}_\lambda$ ($\mathbf{L}_{\text{tot}} = \mathbf{l}_r$) and $\mathbf{S}_{\text{tot}} = \mathbf{S}_{\text{lt}} + \frac{1}{2}$, \mathbf{S}_{lt} is the coupled spin of the light quarks and the number of nodes is $k_{\lambda,\rho}(k_r)$. In addition, in order to unambiguously define these quantum states, we assign to them the flavor \mathcal{F} and spectroscopy $^{2S+1}L_J$ representations. In the following paragraphs, we will construct the possible states for the two different flavor representations available for the charmed baryons, in the energy bands $N = n_\rho + n_\lambda$ ($N = n_r$) and $N = 0, 1, 2$ in order to find S -, P -, D -wave charm-baryon states.

1. The symmetric $\mathbf{6}_f$ -multiplet for the three-quark model

The Ω_c , Ξ'_c , and Σ_c baryons form a flavor sextet in the charm-baryon sector. These charmed baryons have a symmetric flavor-wave function and, in combination with the anti-symmetric color-wave function, the final product wave function is anti-symmetric. This implies that the product of the spatial and spin-wave functions of the light quarks should be symmetric. In the energy band $N = 0$, if $l_\rho = l_\lambda = 0$, the spatial wave function of the two light quarks is symmetric. That is, these states have a symmetric-spin wave function, meaning $\mathbf{S}_{\text{lt}} = \mathbf{1}$. Hence, two ground states, $\mathbf{J}_{\text{tot}} = \mathbf{S}_{\text{tot}} = \mathbf{1}/2, \mathbf{3}/2$, exist. For the energy band $N = 1$, there are two different possibilities. If $l_\rho = 0$ and $l_\lambda = 1$, we again have spatial-symmetric wave functions under the interchange of light quarks, which must be coupled with two possible spin configurations, $\mathbf{S}_{\text{tot}} = \mathbf{1}/2, \mathbf{3}/2$, with $\mathbf{L}_{\text{tot}} = \mathbf{1}$, yielding five P_λ -wave excitations. If $l_\rho = 1$ and $l_\lambda = 0$, the spatial wave function is anti-symmetric under the interchange of light quarks implying that the spin wave function should be anti-symmetric, meaning $\mathbf{S}_{\text{lt}} = \mathbf{0}$, which yields two P_ρ -wave states obtained from $\mathbf{J}_{\text{tot}} = \mathbf{1} + \mathbf{1}/2 = \mathbf{1}/2, \mathbf{3}/2$. In the energy band $N = 2$, when $l_\rho = 0$ and $l_\lambda = 2$, the spatial wave function is

symmetric. Thus, it must be combined with two possible spin configurations, $\mathbf{S}_{\text{tot}} = \mathbf{1}/2, \mathbf{3}/2$, obtaining six D_λ -wave excitations. Additionally, there are radial excitation modes in this band. For the case $k_\rho = 0$ and $k_\lambda = 1$, the spatial wave function is symmetric. Thus the spin wave function must also be symmetric, yielding two λ -radial excitations, $\mathbf{J}_{\text{tot}} = \mathbf{S}_{\text{tot}} = \mathbf{1}/2, \mathbf{3}/2$, since $\mathbf{L}_{\text{tot}} = \mathbf{0}$. The same situation appears when $k_\rho = 1$ and $k_\lambda = 0$; the spatial wave function is symmetric. Thus, there are two ρ -radial excitations, corresponding to $\mathbf{J}_{\text{tot}} = \mathbf{S}_{\text{tot}} = \mathbf{1}/2, \mathbf{3}/2$. In the case $l_\rho = 1$ and $l_\lambda = 1$, which yields $\mathbf{L}_{\text{tot}} = \mathbf{2}, \mathbf{1}, \mathbf{0}$, the product of spatial wave functions is anti-symmetric, implying that we have to couple it with the anti-symmetric spin configurations, $\mathbf{S}_{\text{tot}} = \mathbf{1}/2$, thus obtaining five possible states: two D -wave states, two P -wave states, and one S -wave state. Finally, if $l_\rho = 2$ and $l_\lambda = 0$, the spatial wave functions are symmetric. Hence, we have to combine them with $\mathbf{S}_{\text{tot}} = \mathbf{1}/2, \mathbf{3}/2$, obtaining six D_ρ -wave excitations.

2. The symmetric $\mathbf{6}_f$ -multiplet for the quark-diquark model

When the Ω_c , Ξ'_c , and Σ_c baryons are seen as quark-diquark systems, the two constituent light quarks of the diquark are considered to be correlated, with no internal spatial excitations (S -wave); *i.e.*, it is hypothesized that we are within the limit where the diquark internal spatial excitations are higher in energy than the scale of the resonances studied. Since the hadron must be colorless, the diquark transforms as $\bar{\mathbf{3}}$ under $SU_c(3)$; thus, the product of the spin and flavor wave functions of the diquark configuration should be symmetric. The flavor wave functions of the $\mathbf{6}_f$ representation are symmetric. As a result, we can only combine with axial-vector diquarks; that is, with $\mathbf{S}_{\text{lt}} = \mathbf{1}$. For the energy band $N = 0$, $\mathbf{L}_{\text{tot}} = \mathbf{0}$, and thus $\mathbf{J}_{\text{tot}} = \mathbf{S}_{\text{tot}} = \mathbf{1}/2, \mathbf{3}/2$, yielding two ground states. In the next band $N = 1$, $\mathbf{L}_{\text{tot}} = \mathbf{1}$ has to be coupled with $\mathbf{S}_{\text{tot}} = \mathbf{1}/2, \mathbf{3}/2$, yielding five P -wave excitations. For the band $N = 2$, $\mathbf{L}_{\text{tot}} = \mathbf{2}$, and we must combine with $\mathbf{S}_{\text{tot}} = \mathbf{1}/2, \mathbf{3}/2$, to get six D -wave states. Moreover, there is a radial degree of freedom $k = 1$; with $\mathbf{L}_{\text{tot}} = \mathbf{0}$, we have $\mathbf{J}_{\text{tot}} = \mathbf{S}_{\text{tot}} = \mathbf{1}/2, \mathbf{3}/2$, and hence find two radial excitations.

3. The anti-symmetric $\mathbf{3}_f$ -plet for the three-quark model

The Λ_c and Ξ_c baryons form a flavor-anti-triplet in the charm-baryon sector. These charmed baryons have an anti-symmetric flavor wave function, and which, in combination with the anti-symmetric color wave function, produces a symmetric combination. This implies that the product of the spatial and spin wave functions of the light quarks should be anti-symmetric. For the energy band $N = 0$, if $l_\rho = l_\lambda = 0$, the spatial wave function of the two light quarks is symmetric, thus the spin wave function should be anti-symmetric. This cor-

responds to $\mathbf{S}_{\text{lt}} = \mathbf{0}$, producing only one ground state. For the energy band $N = 1$, if $l_\rho = 0$ and $l_\lambda = 1$, we have a symmetric spatial wave function; thus, the spin wave function should be anti-symmetric. It implies $\mathbf{S}_{\text{tot}} = \mathbf{1}/2$ and, in combination with the total $\mathbf{L}_{\text{tot}} = \mathbf{1}$, yields two P_λ states. If $l_\rho = 1$ and $l_\lambda = 0$, the spatial wave function of the two light quarks is anti-symmetric. Thus, the spin wave function should be symmetric, giving two possible configurations: $\mathbf{S}_{\text{tot}} = \mathbf{1}/2, \mathbf{3}/2$. This, in combination with $\mathbf{L}_{\text{tot}} = \mathbf{1}$, constructs five P_ρ states. In the energy band $N = 2$, in the case of $l_\rho = 0$ and $l_\lambda = 2$, the spatial wave function is symmetric; it is therefore combined with the anti-symmetric spin configuration, $\mathbf{S}_{\text{tot}} = \mathbf{1}/2$, giving two D_λ -wave excitations. The two possible radial excitations, $k_\rho = 0$ and $k_\lambda = 1$, and $k_\rho = 1$ and $k_\lambda = 0$, are symmetric in the spatial wave function. They should be combined with the anti-symmetric spin configuration, $\mathbf{S}_{\text{tot}} = \mathbf{1}/2$, producing one λ -radial excitation and one ρ -radial excitation. The anti-symmetric spatial wave functions of the configuration $l_\rho = 1$ and $l_\lambda = 1$ are coupled to $\mathbf{L}_{\text{tot}} = \mathbf{0}, \mathbf{1}, \mathbf{2}$, and the angular momenta should be combined with the symmetric spin configurations $\mathbf{S}_{\text{tot}} = \mathbf{1}/2, \mathbf{3}/2$, producing thirteen mixed excited states: six D -wave states, five P -wave states, and two S -wave states. Finally, the symmetric configuration $l_\rho = 2$ and $l_\lambda = 0$, combined with the anti-symmetric spin configuration, $\mathbf{S}_{\text{tot}} = \mathbf{1}/2$, gives two D_ρ -wave excitations.

4. The anti-symmetric $\mathbf{3}_f$ -plet for the quark-diquark model

Moreover, Λ_c and Ξ_c baryons are described as quark-diquark systems. In this case, as discussed in subsection II B 2, the diquark presents an S -wave configuration, given its lack of internal spatial excitations. Considering that it is $\mathbf{\bar{3}}$ in the color representation $SU_c(3)$, we conclude that the product of the spin and flavor wave functions of the diquark configuration should be symmetric. In the anti-symmetric $\mathbf{3}_f$ -plet, the flavor wave function is anti-symmetric; thus, the spin wave function of the diquark correspond to a scalar configuration, $\mathbf{S}_{\text{lt}} = \mathbf{0}$. For the energy band $N = 0$, we have $\mathbf{L} = \mathbf{0}$; thus, we only have one ground state $\mathbf{J}_{\text{tot}} = \mathbf{S}_{\text{tot}} = \mathbf{1}/2$. In the next band, $N = 1$, we must combine $\mathbf{L}_{\text{tot}} = \mathbf{1}$ with $\mathbf{S}_{\text{tot}} = \mathbf{1}/2$, which yields two P -wave states. In the band $N = 2$, we have $\mathbf{L}_{\text{tot}} = \mathbf{1}$, and, on coupling to $\mathbf{S}_{\text{tot}} = \mathbf{1}/2$, we get two D -wave states. Finally, with a radial excitation $k_r = 1$ and $\mathbf{L}_{\text{tot}} = \mathbf{0}$, there is only one state.

C. Charmed baryon decay widths

The open-flavor strong decays of a charmed baryon A to another baryon B plus a meson C , $A \rightarrow BC$, have been studied by means of the 3P_0 model [49, 58–60]. According to this model, a $q\bar{q}$ pair is created from the vacuum when a qqc baryon decays and regroups into an outgoing meson and a baryon via the quark rearrangement process

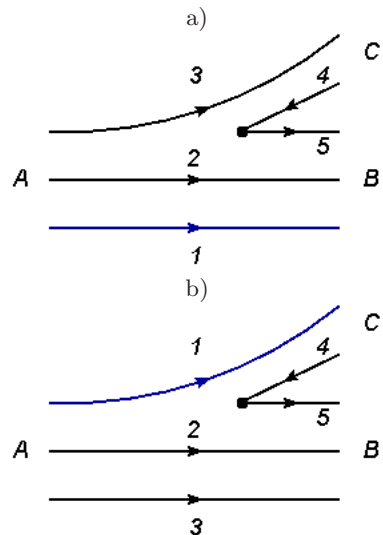


FIG. 1: The 3P_0 pair-creation model. The blue line 1 denotes a charm quark, while the remaining black lines denote light quarks. In diagram a) the charmed baryon A decays to a charmed baryon B and a light meson C . In diagram b) the charmed baryon A decays to a light baryon and a charmed meson C .

as depicted in Fig. 1. In the present study, we consider the decay of a charmed baryon A to a charmed baryon B plus a light meson C , see Fig 1 a), and also the case in which the final state is a light baryon B plus a charmed meson C , see Fig. 1 b). Within the non-relativistic limit, the transition operator is written as

$$T^\dagger = -3\gamma \sum_m \langle 1 m; 1 -m | 0 0 \rangle \int d^3\mathbf{P}_4 d^3\mathbf{P}_5 \delta^3(\mathbf{P}_4 + \mathbf{P}_5) \times \mathcal{Y}_1^m(\mathbf{P}_4 - \mathbf{P}_5) \chi_{1,-m}^{45} \varphi_0^{45} \omega_0^{45} b_{4i}^\dagger(\mathbf{P}_4) d_{5j}^\dagger(\mathbf{P}_5), \quad (6)$$

where 4 and 5 are the indices of the quark and anti-quark created. $\varphi_0^{45} = (u\bar{u} + d\bar{d} + s\bar{s})/\sqrt{3}$ and $\omega_0^{45} = (r\bar{r} + b\bar{b} + g\bar{g})/\sqrt{3}$ are the flavor and color singlet-wave functions, respectively. $\chi_{1,-m}^{45}$ is the spin-triplet state. $\mathcal{Y}_1^m(\mathbf{k}) \equiv |\mathbf{k}| Y_1^m(\theta_k, \phi_k)$ is a solid harmonic polynomial corresponding to the P -wave quark pair. γ_0 is a dimensionless constant related to the strength of the $q\bar{q}$ pair creation vertex from the vacuum. γ_0 is a free parameter of the 3P_0 model.

The total decay width Γ is the sum of the partial widths for the open channels BC , $\Gamma = \sum_{BC} \Gamma_{A \rightarrow BC}$, where the partial widths $\Gamma_{A \rightarrow BC}$, are computed as

$$\Gamma_{A \rightarrow BC} = \frac{2\pi\gamma_0^2}{2J_A + 1} \Phi_{A \rightarrow BC}(q_0) \times \sum_{M_{J_A}, M_{J_B}} |\mathcal{M}^{M_{J_A}, M_{J_B}}|^2. \quad (7)$$

Here, $\mathcal{M} = \langle BC | T^\dagger | A \rangle$ is the 3P_0 amplitude written in terms of hadron h.o. wave functions and the sum runs

over the projections M_{J_A, J_B} of the total angular momenta $J_{A, B}$ of A and B . q_0 is the relative momentum between B and C , and the coefficient $\Phi_{A \rightarrow BC}(q_0)$ is the relativistic phase space factor [60],

$$\Phi_{A \rightarrow BC}(q_0) = q_0 \frac{E_B(q_0)E_C(q_0)}{m_A},$$

$$\text{with } E_{B, C} = \sqrt{m_{B, C}^2 + q_0^2};$$

where m_A is the initial charmed baryon mass in its rest frame. The masses m_B and m_C and energies E_B and E_C correspond to the final baryon and meson, respectively.

The h.o. wave functions depend on the parameters $\alpha_{\rho(\lambda)}$, see A, which, in Reference [60], are regarded as free parameters. Conversely, in the present study, $\alpha_{\rho(\lambda)}$ are related to the baryon ρ - and λ -mode h.o. frequencies as defined in Eq. 3; this relation is established by $\alpha_{\rho(\lambda)}^2 = \omega_{\rho(\lambda)} m_{\rho(\lambda)}$. Therefore, $\alpha_{\rho(\lambda)}$ will depend on the fit parameter K_c and constituent quark masses. The h.o. wave functions and coordinate system conventions used in our decay width calculations are given in A. The decay widths are calculated for each charm-baryon type; the available open-flavor channels include all the pseudoscalar and vector mesons. The open-flavor channels share an extra parameter R related to the meson size, which has been discussed extensively in the literature [61–63]; we adopt $R = 2.1/\text{GeV}$ which is taken from References [49, 64]. The flavor-meson-wave functions are given in D. All the possible flavor couplings, $\mathcal{F}_{A \rightarrow BC} = \langle \phi_B \phi_C | \phi_0 \phi_A \rangle$ are given in E. The masses of the decay products are listed in Table XIV in G. It is important to mention that the application of the 3P_0 model is restricted to the three-quark system, owing the difficulty of dealing with diquark spatial wave functions within the 3P_0 model formalism.

III. PARAMETER DETERMINATION AND UNCERTAINTIES

A. Mass spectra of charmed baryons

We fitted a selection of experimentally observed charm-baryon states, Ω_c , Σ_c , Λ_c , Ξ'_c , and Ξ_c , to the masses predicted by Eq. 2 and Eq. 4 to obtain the constituent quark and diquark masses (m_c , m_s , $m_{u, d}$, $m_{D\Omega}$, $m_{D\Xi}$, and $m_{D\Sigma, \Lambda}$) and the model parameters (P_s , P_{sl} , P_I , P_f and K_c). The fitted model parameters and masses minimize the sum of the squared differences between the experimental baryon masses and those predicted by the model (least-squares method).

The measured baryon masses come with statistical and systematic uncertainties. Furthermore, the models in Eq. 2 and Eq. 4 are approximate descriptions of the charm baryons. Thus, to take into account the possible deviations of these models from the experimental observations, we assigned a model uncertainty to each model.

Parameter	three-quark	diquark
	Value	Value
m_c	$1606.15^{+57.82}_{-61.2}$ MeV	$1562.94^{+22.65}_{-24.38}$ MeV
m_s	$455.31^{+29.24}_{-26.76}$ MeV	†
$m_{u, d}$	$283.91^{+30.03}_{-30.93}$ MeV	†
$m_{D\Omega}$	†	$947.05^{+2.95}_{-2.95}$ MeV
$m_{D\Xi}$	†	$790.85^{+17.52}_{-14.34}$ MeV
$m_{D\Sigma, \Lambda}$	†	$612.98^{+19.55}_{-16.79}$ MeV
K_c	$0.029^{+0.0007}_{-0.0008}$ GeV ³	$0.0195^{+0.0007}_{-0.0007}$ GeV ³
P_s	$23.07^{+3.16}_{-3.1}$ MeV	$24.27^{+3.09}_{-3.11}$ MeV
P_{sl}	$18.02^{+5.39}_{-5.4}$ MeV	$16.92^{+5.38}_{-5.3}$ MeV
P_I	$45.15^{+8.47}_{-8.43}$ MeV	$41.22^{+8.8}_{-8.74}$ MeV
P_f	$52.42^{+5.75}_{-5.74}$ MeV	$52.34^{+6.58}_{-6.61}$ MeV

TABLE I: Fitted parameters for the three-quark model (second column) and the quark-diquark model (third column). The † indicates that the parameter is absent in that model.

The model uncertainty, σ_{mod} , is calculated in accordance with Ref. [9] and is such that $\chi^2/NDF \simeq 1$, where

$$\chi^2 = \sum_i \frac{(M_{mod, i} - M_{exp, i})^2}{\sigma_{mod}^2 + \sigma_{exp, i}^2}, \quad (8)$$

$M_{mod, i}$ are the predicted charm baryon masses, $M_{exp, i}$ are the experimental charm baryon masses included in the fit with uncertainties $\sigma_{exp, i}$, and NDF is the number of degrees of freedom. We obtained $\sigma_{mod} = 15.42$ MeV for the three-quark model and $\sigma_{mod} = 13.63$ MeV for the quark-diquark model.

To integrate the experimental and model uncertainties into our fit, we carried out a statistical simulation of error propagation. To do so, we randomly sampled the experimental masses from a Gaussian shaped distribution with a mean equal to the central mass value and a width equal to the squared sum of the uncertainties. We fitted the model by using a sampled mass corresponding to each experimental observed state included in the fit, and we repeated the procedure 10^4 times. In this manner, we obtained a Gaussian distribution for each constituent quark mass, model parameter, and the baryon mass itself. Next, we assigned the mean of the distribution as the value of the parameter and used its difference from the distribution quantiles at 68% confidence level (C.L.), in order to extract the uncertainty. This method is known as the Monte Carlo bootstrap uncertainty propagation [55, 65].

The experimental masses and their corresponding uncertainties used in the fit and error propagation are marked with (*) in Tables IV–VII. These mass measurements are summarized in the PDG database [9]. However, the charm-baryon masses predicted by Eq. 2 are degenerated in comparison with different u or d quark configurations, since the model will assign identical masses to baryons with the same number of u or d quark contents. This is a consequence of isospin symmetry. That is to say,

the Σ_c baryons are measured in the states $\Sigma_c^{++} = uuc$, $\Sigma_c^+ = udc$ and $\Sigma_c^0 = ddc$, which display small mass differences. These three states are degenerated in our model. Additionally, the same situation emerges for the states $\Xi_c^+ = usc$ and $\Xi_c^0 = dsc$, which are taken as the Ξ_c baryons. As these groups of mass states have the same quantum numbers, our quantum number assignments are not affected by the mass degeneracy. In our calculations, to account for this degeneracy, we fitted the arithmetic mean of the measured masses and adopted a conservative approach to the uncertainty by defining it as the standard deviation among the measured masses, plus their highest reported experimental uncertainty. The calculations were carried out by using MINUIT [66] and NumPy [67]. The results of the fit are shown in Table I. The constituent quark masses obtained agree with previous theoretical determinations [13]. Furthermore, the model parameters used in the present study are in the range of our previous work [53], where phenomenological considerations were considered to determine them. Tables II and III show the correlation of the fitted parameters in the three-quark and quark-diquark model, respectively. In the three-quark model, the constituent quark masses are highly correlated, indicating that the quark masses exhibit similar behavior inside the baryon. Moreover, the spring constant K_c is also highly correlated with the quark masses, as expected from Eq. 3. In the quark-diquark model, the charm-quark mass is totally uncorrelated with the diquark masses; this is a consequence of the diatomic structure of the modeled baryon. In the same manner, K_c is correlated with the diquark masses, as expected from Eq. 5.

	m_c	m_s	m_n	K_c	P_s	P_{sl}	P_I	P_f
m_c	1							
m_s	-0.76	1						
$m_{u,d}$	-0.82	0.76	1					
K_c	-0.77	0.7	0.69	1				
P_s	0.26	-0.29	-0.27	-0.14	1			
P_{sl}	-0.1	0.08	0.08	0.37	-0.21	1		
P_I	0.11	0.12	-0.19	-0.16	0.21	-0.02	1	
P_f	-0.42	0.04	0.28	0.36	-0.51	0.21	-0.68	1

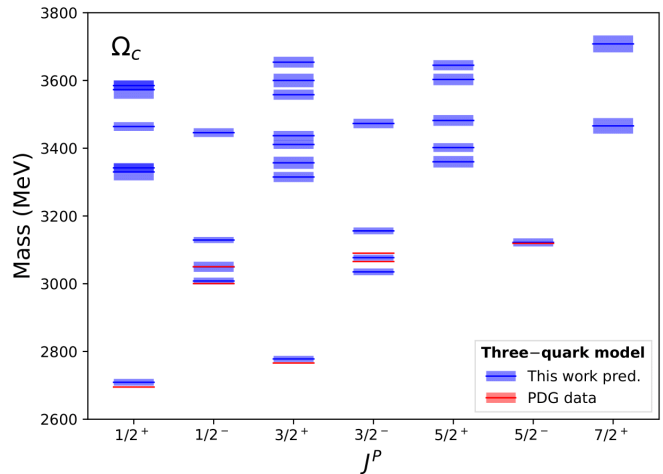
TABLE II: Correlation between fitted parameters: three-quark system.

B. Charm-baryon decay widths

Parameter determination and error propagation for the decay widths were carried out in analogy with the above procedure for the charm-baryon masses. The pair-creation constant γ_0 of Eq. 7 was obtained by fitting data of selected charm-baryon decay widths.

To compute the uncertainty of the decay widths, we considered all possible sources of uncertainty. First, the

FIG. 2: Ω_c mass spectra and tentative quantum number assignments on using the three-quark model. The theoretical predictions and their uncertainties (blue lines and bands) are compared with the experimental results (red lines and bands) reported in the PDG [9]. The experimental errors are too small to be evaluated on this energy scale.



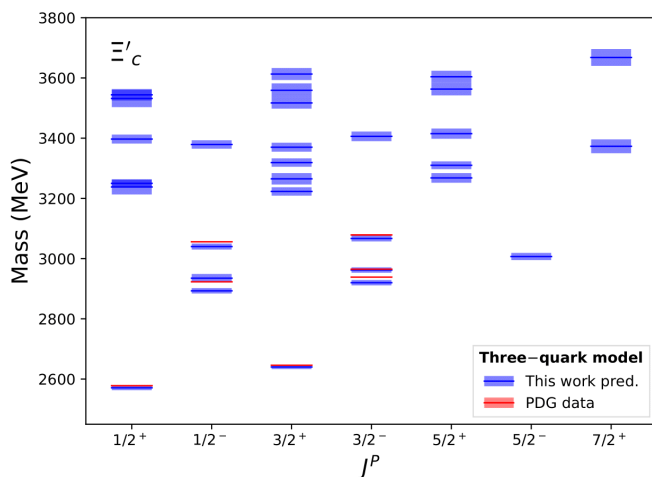
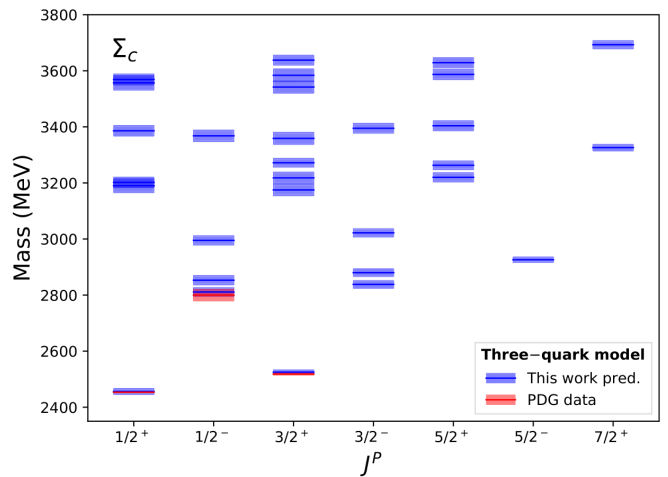
error coming from the baryon mass m_A and parameter K_c were included by calculating a decay width for all the statistically simulated constituent quark masses, m_A and K_c and γ_0 ; each width calculation was then repeated 10^4 times. Next, we included the experimental uncertainties of the decay products m_B and m_C . These experimental uncertainties, the values of which are shown in Table XIV, were propagated to the decay widths by means of the same random sampling technique described for the masses. Furthermore, a model uncertainty, $\sigma_{mod} = 4.44$, was included. We set the decay width value as the population mean of the Gaussian distribution obtained, with an error equivalent to the difference between this mean and the distribution quantiles at 68% C.L. The value and uncertainty obtained are $\gamma_0 = 19.6 \pm 5.1$. These calculations are only performed when the charmed baryons are modeled as three-quark systems.

IV. RESULTS AND DISCUSSION

In this section, we present our results regarding the mass spectra and total decay widths of charmed baryons. The mass spectra are computed via the mass formula of Eq. 1. The theoretical masses and their uncertainties are reported in the third column for the three-quark system and in the fourth column for the quark-diquark system in Tables IV-VIII. The theoretical decay widths for the three-quark system are computed by using the 3P_0 model described in Sec. II C. Each open-flavor channel decay width is obtained via Eq. 7, and the total decay width is the sum over all the channels. The theoretical total-decay widths and their uncertainties for the three-quark

	m_c	m_{D_Ω}	m_{D_Ξ}	$m_{D_{\Sigma,\Lambda}}$	K_c	P_s	P_{sl}	P_I	P_f
m_c	1								
m_{D_Ω}	0.0	1							
m_{D_Ξ}	0.0	0.85	1						
$m_{D_{\Sigma,\Lambda}}$	0.0	-0.83	0.3	1					
K_c	0.0	0.33	0.3	-0.52	1				
P_s	0.0	-0.18	-0.1	0.18	-0.14	1			
P_{sl}	0.0	0.14	0.1	-0.18	0.37	-0.21	1		
P_I	0.0	-0.72	-0.78	0.63	-0.16	0.21	-0.02	1	
P_f	0.0	0.7	0.68	-0.88	0.36	-0.51	0.21	-0.68	1

TABLE III: Correlation between fitted parameters: quark-diquark system.

FIG. 3: As Figure 2, but for Ξ'_c resonances.FIG. 4: As Figure 2, but for Σ_c resonances.

system are reported in the fifth column of Tables IV-VIII. The partial-decay widths to all open-flavor channels are found in Tables IX-XIII of F.

Our proposed quantum number assignments for the charm-baryon states are summarized in Figures 2-6 within the three-quark model. There is a good agreement between the predicted mass pattern spectrum and the experimental data. Furthermore, we present our charm-baryon spectrum on using the quark-diquark framework in Figures 7-11. In the following subsections, we discuss our assignments to the available data reported in the PDG [9].

A. Assignments of charmed baryons

First, we discuss our assignments based on our theoretical analyses of the charmed baryons Ω_c , Ξ'_c , Σ_c , Ξ_c , and Λ_c . As a first criterion, we use our mass spectrum to identify the charm-baryon resonances, and the decay width as a secondary criterion. The classification for the quark-diquark model is equivalent to that of the three-

quark model when we describe ground states and λ -type excitations. When states are identified as ρ -type excitations in the three-quark model, there are no equivalent states in the quark-diquark model (see Tables IV-VIII).

1. Ω_c

Our results for the Ω_c resonances are reported in Table IV; they are in good agreement with the experimental masses reported in the PDG [9]. Our results are also consistent with our previous calculations [53]. Here we have extended our calculations up to D -wave states. The Ω_c and $\Omega_c(2770)$ states are well reproduced in our model. They are identified as the ground states with quantum numbers (QN) $J^P = 1/2^+$ and $J^P = 3/2^+$; note that these QN have not been yet measured. The observed $\Omega_c(3000)$ resonance could be identified as a P_λ -wave state with $J^P = 1/2^-$, where the total-internal-spin is $S = 1/2$; our theoretical width is compatible with the experimental value. The $\Omega_c(3050)$ has an excellent match in our model; the mass is well reproduced, but the width is slightly overestimated; the $\Omega_c(3050)$ is iden-

$\Omega_c(ssc)$ $\mathcal{F} = \mathbf{6}_f$		Three-quark Quark-diquark				
		Predicted Mass (MeV)	Predicted Mass (MeV)	Experimental Mass (MeV)	Predicted Γ_{tot} (MeV)	Experimental Γ (MeV)
$N = 0$						
$ l_\lambda=0, l_\rho=0, k_\lambda=0, k_\rho=0\rangle$	${}^2S_{1/2}$	2709^{+10}_{-10}	2702^{+9}_{-9}	2695.0 ± 1.7 (*)	$0.0^{+0.0}_{-0.0}$	$< 10^{-7}$
$ l_\lambda=0, l_\rho=0, k_\lambda=0, k_\rho=0\rangle$	${}^4S_{3/2}$	2778^{+9}_{-9}	2776^{+9}_{-9}	2765.9 ± 2.0 (*)	$0.0^{+0.0}_{-0.0}$	\dagger
$N = 1$						
$ l_\lambda=1, l_\rho=0, k_\lambda=0, k_\rho=0\rangle$	${}^2P_{1/2}$	3008^{+10}_{-10}	3000^{+9}_{-9}	3000.4 ± 0.22 (*)	$4.1^{+2.0}_{-2.0}$	$4.5 \pm 0.6 \pm 0.3$ (*)
$ l_\lambda=1, l_\rho=0, k_\lambda=0, k_\rho=0\rangle$	${}^4P_{1/2}$	3050^{+15}_{-15}	3048^{+14}_{-14}	3050.2 ± 0.13	$7.5^{+3.7}_{-3.7}$	$0.8 \pm 0.2 \pm 0.1$
$ l_\lambda=1, l_\rho=0, k_\lambda=0, k_\rho=0\rangle$	${}^2P_{3/2}$	3035^{+10}_{-10}	3025^{+10}_{-10}	3065.6 ± 0.28	$26.3^{+12.9}_{-12.9}$	$3.5 \pm 0.4 \pm 0.2$
$ l_\lambda=1, l_\rho=0, k_\lambda=0, k_\rho=0\rangle$	${}^4P_{3/2}$	3077^{+9}_{-9}	3073^{+8}_{-8}	3090.2 ± 0.5	$6.6^{+3.3}_{-3.3}$	$8.7 \pm 1.0 \pm 0.8$
$ l_\lambda=1, l_\rho=0, k_\lambda=0, k_\rho=0\rangle$	${}^4P_{5/2}$	3122^{+12}_{-12}	3115^{+12}_{-11}	3119.1 ± 1.0 (*)	$50.0^{+24.7}_{-24.3}$	60 ± 26 (*)
$ l_\lambda=0, l_\rho=1, k_\lambda=0, k_\rho=0\rangle$	${}^2P_{1/2}$	3129^{+9}_{-9}	$\dagger\dagger$	\dagger	$14.4^{+1.6}_{-9.5}$	\dagger
$ l_\lambda=0, l_\rho=1, k_\lambda=0, k_\rho=0\rangle$	${}^2P_{3/2}$	3156^{+10}_{-10}	$\dagger\dagger$	\dagger	$71.6^{+36.1}_{-35.2}$	\dagger
$N = 2$						
$ l_\lambda=2, l_\rho=0, k_\lambda=0, k_\rho=0\rangle$	${}^2D_{3/2}$	3315^{+15}_{-14}	3306^{+14}_{-14}	\dagger	$10.6^{+5.3}_{-5.3}$	\dagger
$ l_\lambda=2, l_\rho=0, k_\lambda=0, k_\rho=0\rangle$	${}^2D_{5/2}$	3360^{+17}_{-16}	3348^{+17}_{-17}	\dagger	$24.4^{+12.0}_{-11.9}$	\dagger
$ l_\lambda=2, l_\rho=0, k_\lambda=0, k_\rho=0\rangle$	${}^4D_{1/2}$	3330^{+25}_{-25}	3328^{+24}_{-23}	\dagger	$16.3^{+8.2}_{-8.0}$	\dagger
$ l_\lambda=2, l_\rho=0, k_\lambda=0, k_\rho=0\rangle$	${}^4D_{3/2}$	3357^{+18}_{-19}	3354^{+17}_{-17}	\dagger	$30.4^{+14.8}_{-14.9}$	\dagger
$ l_\lambda=2, l_\rho=0, k_\lambda=0, k_\rho=0\rangle$	${}^4D_{5/2}$	3402^{+13}_{-13}	3396^{+12}_{-12}	\dagger	$62.3^{+31.0}_{-31.1}$	\dagger
$ l_\lambda=2, l_\rho=0, k_\lambda=0, k_\rho=0\rangle$	${}^4D_{7/2}$	3466^{+23}_{-23}	3455^{+23}_{-23}	\dagger	$123.0^{+61.4}_{-62.1}$	\dagger
$ l_\lambda=0, l_\rho=0, k_\lambda=1, k_\rho=0\rangle$	${}^2S_{1/2}$	3342^{+14}_{-14}	3331^{+15}_{-15}	\dagger	$1.3^{+0.6}_{-0.6}$	\dagger
$ l_\lambda=0, l_\rho=0, k_\lambda=1, k_\rho=0\rangle$	${}^4S_{3/2}$	3411^{+13}_{-13}	3404^{+12}_{-12}	\dagger	$3.2^{+1.6}_{-1.6}$	\dagger
$ l_\lambda=0, l_\rho=0, k_\lambda=0, k_\rho=1\rangle$	${}^2S_{1/2}$	3585^{+15}_{-15}	$\dagger\dagger$	\dagger	$18.3^{+9.2}_{-9.2}$	\dagger
$ l_\lambda=0, l_\rho=0, k_\lambda=0, k_\rho=1\rangle$	${}^4S_{3/2}$	3654^{+16}_{-16}	$\dagger\dagger$	\dagger	$24.0^{+12.1}_{-12.0}$	\dagger
$ l_\lambda=1, l_\rho=1, k_\lambda=0, k_\rho=0\rangle$	${}^2D_{3/2}$	3437^{+14}_{-14}	$\dagger\dagger$	\dagger	$198.0^{+97.9}_{-98.0}$	\dagger
$ l_\lambda=1, l_\rho=1, k_\lambda=0, k_\rho=0\rangle$	${}^2D_{5/2}$	3482^{+16}_{-16}	$\dagger\dagger$	\dagger	$114.9^{+56.6}_{-56.3}$	\dagger
$ l_\lambda=1, l_\rho=1, k_\lambda=0, k_\rho=0\rangle$	${}^2P_{1/2}$	3446^{+13}_{-13}	$\dagger\dagger$	\dagger	$2.1^{+1.1}_{-1.0}$	\dagger
$ l_\lambda=1, l_\rho=1, k_\lambda=0, k_\rho=0\rangle$	${}^2P_{3/2}$	3473^{+14}_{-14}	$\dagger\dagger$	\dagger	$3.1^{+1.5}_{-1.5}$	\dagger
$ l_\lambda=1, l_\rho=1, k_\lambda=0, k_\rho=0\rangle$	${}^2S_{1/2}$	3464^{+13}_{-13}	$\dagger\dagger$	\dagger	$88.2^{+43.1}_{-44.0}$	\dagger
$ l_\lambda=0, l_\rho=2, k_\lambda=0, k_\rho=0\rangle$	${}^2D_{3/2}$	3558^{+15}_{-15}	$\dagger\dagger$	\dagger	$217.1^{+108.6}_{-107.4}$	\dagger
$ l_\lambda=0, l_\rho=2, k_\lambda=0, k_\rho=0\rangle$	${}^2D_{5/2}$	3603^{+17}_{-17}	$\dagger\dagger$	\dagger	$174.3^{+85.1}_{-86.0}$	\dagger
$ l_\lambda=0, l_\rho=2, k_\lambda=0, k_\rho=0\rangle$	${}^4D_{1/2}$	3573^{+27}_{-26}	$\dagger\dagger$	\dagger	$217.6^{+140.3}_{-138.5}$	\dagger
$ l_\lambda=0, l_\rho=2, k_\lambda=0, k_\rho=0\rangle$	${}^4D_{3/2}$	3600^{+20}_{-20}	$\dagger\dagger$	\dagger	$284.8^{+144.4}_{-144.7}$	\dagger
$ l_\lambda=0, l_\rho=2, k_\lambda=0, k_\rho=0\rangle$	${}^4D_{5/2}$	3645^{+15}_{-16}	$\dagger\dagger$	\dagger	$212.0^{+102.7}_{-103.8}$	\dagger
$ l_\lambda=0, l_\rho=2, k_\lambda=0, k_\rho=0\rangle$	${}^4D_{7/2}$	3708^{+25}_{-25}	$\dagger\dagger$	\dagger	$383.1^{+191.8}_{-193.9}$	\dagger

TABLE IV: $\Omega_c(ssc)$ resonances. The flavor content is specified with an \mathcal{F} . The first column shows the quantum states $|l_\lambda(l_r), l_\rho, k_\lambda(k_r), k_\rho\rangle$ for the three-quark (quark-diquark) model, where $l_{\lambda,\rho}(l_r)$ are the orbital angular momenta and $k_{\lambda,\rho}(k_r)$ the number of nodes of the $\lambda(r)$ and ρ oscillators. Furthermore, $N = n_\rho + n_\lambda$ ($N = n_r$) separate the energy bands $N = 0, 1, 2$. The second column contains the spectroscopic notation ${}^{2S+1}L_J$ for each state and is defined by the total angular momentum $\mathbf{J}_{tot} = \mathbf{L}_{tot} + \mathbf{S}_{tot}$, where $\mathbf{S}_{tot} = \mathbf{S}_{it} + \frac{1}{2}$, and $\mathbf{L}_{tot} = \mathbf{l}_\rho + \mathbf{l}_\lambda$ ($\mathbf{L}_{tot} = \mathbf{l}_r$, for the quark-diquark model). The predicted masses, computed within the three-quark model, are shown in the third column, whereas their corresponding total strong decay widths are shown in the sixth column. The predicted masses, computed within the quark-diquark framework, are presented in the fourth column. Our theoretical results are compared with the experimental masses of the fifth column and the total decay widths of the seventh column [1, 68]. The (*) indicate the experimental mass and decay width values included in the fits. The \dagger indicates that there is no reported experimental mass or decay for that state. The $\dagger\dagger$ indicates that there is no quark-diquark prediction for that state.

tified as the $J^P = 1/2^-$ state, with total-internal-spin $S = 3/2$. In our calculations, the central value deviates 20 MeV for $\Omega_c(3065)$; however, the width is overestimated. Hence, we identify the observed $\Omega_c(3065)$ as the

state $J^P = 3/2^-$ with internal-total-spin $S = 1/2$. It should be noted that our state $J^P = 3/2^-$ is lighter in mass than the state $J^P = 1/2^-$; this may be a numerical consequence of the fit. However, this opens the possi-

$\Sigma_c(nnc)$		Three-quark Quark-diquark				
$\mathcal{F} = \mathbf{6}_f$	$2S+1L_J$	Predicted Mass (MeV)	Predicted Mass (MeV)	Experimental Mass (MeV)	Predicted Γ_{tot} (MeV)	Experimental Γ (MeV)
$N = 0$						
$ l_\lambda=0, l_\rho=0, k_\lambda=0, k_\rho=0\rangle$	${}^2S_{1/2}$	2456^{+11}_{-11}	2451^{+11}_{-11}	2453.5 ± 0.9 (*)	$1.7^{+1.1}_{-1.2}$	$2.3 \pm 0.3 \pm 0.3$ (*)
$ l_\lambda=0, l_\rho=0, k_\lambda=0, k_\rho=0\rangle$	${}^4S_{3/2}$	2525^{+11}_{-11}	2524^{+11}_{-11}	2518.1 ± 2.8 (*)	$14.9^{+7.8}_{-7.9}$	$17.2 \pm 2.3 \pm 3.1$ (*)
$N = 1$						
$ l_\lambda=1, l_\rho=0, k_\lambda=0, k_\rho=0\rangle$	${}^2P_{1/2}$	2811^{+12}_{-12}	2798^{+14}_{-14}	2800.0 ± 20.0 (*)	$30.5^{+17.5}_{-17.1}$	75 ± 60 (*)
$ l_\lambda=1, l_\rho=0, k_\lambda=0, k_\rho=0\rangle$	${}^4P_{1/2}$	2853^{+17}_{-17}	2845^{+18}_{-18}	†	$61.2^{+31.2}_{-30.4}$	†
$ l_\lambda=1, l_\rho=0, k_\lambda=0, k_\rho=0\rangle$	${}^2P_{3/2}$	2838^{+12}_{-13}	2823^{+15}_{-15}	†	$182.6^{+91.8}_{-90.1}$	†
$ l_\lambda=1, l_\rho=0, k_\lambda=0, k_\rho=0\rangle$	${}^4P_{3/2}$	2880^{+13}_{-13}	2871^{+13}_{-13}	†	$165.1^{+79.6}_{-79.3}$	†
$ l_\lambda=1, l_\rho=0, k_\lambda=0, k_\rho=0\rangle$	${}^4P_{5/2}$	2925^{+16}_{-16}	2913^{+16}_{-16}	†	$236.6^{+115.3}_{-116.2}$	†
$ l_\lambda=0, l_\rho=1, k_\lambda=0, k_\rho=0\rangle$	${}^2P_{1/2}$	2994^{+16}_{-17}	††	†	$124.6^{+60.6}_{-60.3}$	†
$ l_\lambda=0, l_\rho=1, k_\lambda=0, k_\rho=0\rangle$	${}^2P_{3/2}$	3021^{+17}_{-17}	††	†	$125.0^{+63.0}_{-61.1}$	†
$N = 2$						
$ l_\lambda=2, l_\rho=0, k_\lambda=0, k_\rho=0\rangle$	${}^2D_{3/2}$	3175^{+17}_{-17}	3153^{+21}_{-21}	†	$154.9^{+77.8}_{-79.0}$	†
$ l_\lambda=2, l_\rho=0, k_\lambda=0, k_\rho=0\rangle$	${}^2D_{5/2}$	3220^{+19}_{-19}	3195^{+23}_{-23}	†	$249.7^{+123.7}_{-121.8}$	†
$ l_\lambda=2, l_\rho=0, k_\lambda=0, k_\rho=0\rangle$	${}^4D_{1/2}$	3190^{+28}_{-27}	3175^{+28}_{-28}	†	$102.3^{+50.9}_{-51.4}$	†
$ l_\lambda=2, l_\rho=0, k_\lambda=0, k_\rho=0\rangle$	${}^4D_{3/2}$	3217^{+22}_{-22}	3201^{+23}_{-23}	†	$154.4^{+75.5}_{-75.3}$	†
$ l_\lambda=2, l_\rho=0, k_\lambda=0, k_\rho=0\rangle$	${}^4D_{5/2}$	3262^{+18}_{-18}	3243^{+19}_{-20}	†	$236.4^{+114.6}_{-113.9}$	†
$ l_\lambda=2, l_\rho=0, k_\lambda=0, k_\rho=0\rangle$	${}^4D_{7/2}$	3326^{+26}_{-26}	3302^{+28}_{-28}	†	$457.7^{+223.6}_{-224.5}$	†
$ l_\lambda=0, l_\rho=0, k_\lambda=1, k_\rho=0\rangle$	${}^2S_{1/2}$	3202^{+17}_{-17}	3178^{+21}_{-21}	†	$6.8^{+3.4}_{-3.3}$	†
$ l_\lambda=0, l_\rho=0, k_\lambda=1, k_\rho=0\rangle$	${}^4S_{3/2}$	3271^{+18}_{-18}	3251^{+20}_{-20}	†	$6.1^{+3.0}_{-3.0}$	†
$ l_\lambda=0, l_\rho=0, k_\lambda=0, k_\rho=1\rangle$	${}^2S_{1/2}$	3567^{+31}_{-31}	††	†	$18.6^{+9.6}_{-9.5}$	†
$ l_\lambda=0, l_\rho=0, k_\lambda=0, k_\rho=1\rangle$	${}^4S_{3/2}$	3637^{+33}_{-33}	††	†	$25.8^{+13.0}_{-13.2}$	†
$ l_\lambda=1, l_\rho=1, k_\lambda=0, k_\rho=0\rangle$	${}^2D_{3/2}$	3358^{+22}_{-23}	††	†	$386.4^{+189.1}_{-189.4}$	†
$ l_\lambda=1, l_\rho=1, k_\lambda=0, k_\rho=0\rangle$	${}^2D_{5/2}$	3403^{+24}_{-24}	††	†	$333.6^{+173.7}_{-171.5}$	†
$ l_\lambda=1, l_\rho=1, k_\lambda=0, k_\rho=0\rangle$	${}^2P_{1/2}$	3367^{+22}_{-22}	††	†	$7.9^{+5.7}_{-5.7}$	†
$ l_\lambda=1, l_\rho=1, k_\lambda=0, k_\rho=0\rangle$	${}^2P_{3/2}$	3394^{+23}_{-23}	††	†	$32.4^{+28.9}_{-28.3}$	†
$ l_\lambda=1, l_\rho=1, k_\lambda=0, k_\rho=0\rangle$	${}^2S_{1/2}$	3385^{+22}_{-23}	††	†	$99.9^{+52.3}_{-52.3}$	†
$ l_\lambda=0, l_\rho=2, k_\lambda=0, k_\rho=0\rangle$	${}^2D_{3/2}$	3540^{+31}_{-31}	††	†	$476.0^{+229.4}_{-226.0}$	†
$ l_\lambda=0, l_\rho=2, k_\lambda=0, k_\rho=0\rangle$	${}^2D_{5/2}$	3585^{+32}_{-32}	††	†	$722.2^{+368.9}_{-370.5}$	†
$ l_\lambda=0, l_\rho=2, k_\lambda=0, k_\rho=0\rangle$	${}^4D_{1/2}$	3555^{+39}_{-39}	††	†	$1150.0^{+565.0}_{-557.5}$	†
$ l_\lambda=0, l_\rho=2, k_\lambda=0, k_\rho=0\rangle$	${}^4D_{3/2}$	3582^{+35}_{-35}	††	†	$651.6^{+318.5}_{-313.2}$	†
$ l_\lambda=0, l_\rho=2, k_\lambda=0, k_\rho=0\rangle$	${}^4D_{5/2}$	3627^{+33}_{-33}	††	†	$412.3^{+206.6}_{-206.0}$	†
$ l_\lambda=0, l_\rho=2, k_\lambda=0, k_\rho=0\rangle$	${}^4D_{7/2}$	3691^{+38}_{-38}	††	†	$1879.4^{+976.6}_{-973.8}$	†

TABLE V: As Table IV, but for $\Sigma_c(nnc)$ resonances.

bility of interchanging the assignments of the $\Omega_c(3050)$ and $\Omega_c(3065)$ states, with $J^P = 3/2^-$ and $J^P = 1/2^-$, respectively. Only future experiments will confirm the right order and unique assignments. The $\Omega_c(3090)$ is identified as the state $J^P = 3/2^-$ with spin $S = 3/2$; however, its theoretical mass is slightly underestimated, but the theoretical width is in good agreement with the experimental value. Finally, the mass and width of the $\Omega_c(3120)$ resonance is well reproduced in our model; it is identified as the state $J^P = 5/2^-$ with spin $S = 3/2$. This state was not confirmed by Belle [2], other interpretations are therefore possible. Since this state is very narrow, it can be described as a molecular state [53].

2. Σ_c

Our results for Σ_c states are reported in Table V. There are only three experimentally observed Σ_c states, all of which have masses that are in excellent agreement with our predictions. $\Sigma_c(2455)$ is identified as the ground state $J^P = 1/2^+$. The quantum numbers have not yet been measured, and our theoretical mass is in good agreement with the experimental mass and our theoretical width is in good agreement with the experimental width. We find a similar situation in the case of $\Sigma_c(2520)$, which is identified as a ground state with a spin excitation $J^P = 3/2^+$. The quantum numbers have not yet been measured, but

$\Xi'_c(snc)$ $\mathcal{F} = \mathbf{6}_f$		Three-quark Quark-diquark				
		Predicted Mass (MeV)	Predicted Mass (MeV)	Experimental Mass (MeV)	Predicted Γ_{tot} (MeV)	Experimental Γ (MeV)
$N = 0$						
$ l_\lambda=0, l_\rho=0, k_\lambda=0, k_\rho=0\rangle$	${}^2S_{1/2}$	2571^{+8}_{-8}	2577^{+10}_{-10}	2578.0 ± 0.9 (*)	$0.0^{+0.0}_{-0.0}$	†
$ l_\lambda=0, l_\rho=0, k_\lambda=0, k_\rho=0\rangle$	${}^4S_{3/2}$	2640^{+7}_{-7}	2650^{+9}_{-9}	2645.9 ± 0.71 (*)	$0.4^{+0.2}_{-0.2}$	2.25 ± 0.41 (*)
$N = 1$						
$ l_\lambda=1, l_\rho=0, k_\lambda=0, k_\rho=0\rangle$	${}^2P_{1/2}$	2893^{+9}_{-9}	2893^{+11}_{-11}	†	$7.3^{+3.6}_{-3.5}$	†
$ l_\lambda=1, l_\rho=0, k_\lambda=0, k_\rho=0\rangle$	${}^4P_{1/2}$	2935^{+14}_{-15}	2941^{+14}_{-14}	2923.0 ± 0.35	$5.0^{+2.4}_{-2.5}$	7.1 ± 2.0
$ l_\lambda=1, l_\rho=0, k_\lambda=0, k_\rho=0\rangle$	${}^2P_{3/2}$	2920^{+9}_{-9}	2919^{+13}_{-13}	2938.5 ± 0.3	$28.0^{+13.9}_{-13.7}$	15 ± 9
$ l_\lambda=1, l_\rho=0, k_\lambda=0, k_\rho=0\rangle$	${}^4P_{3/2}$	2962^{+9}_{-9}	2966^{+10}_{-10}	2964.9 ± 0.33 (*)	$18.9^{+9.0}_{-9.2}$	14.1 ± 1.6 (*)
$ l_\lambda=1, l_\rho=0, k_\lambda=0, k_\rho=0\rangle$	${}^4P_{5/2}$	3007^{+12}_{-12}	3009^{+14}_{-14}	†	$43.1^{+20.8}_{-21.1}$	†
$ l_\lambda=0, l_\rho=1, k_\lambda=0, k_\rho=0\rangle$	${}^2P_{1/2}$	3040^{+10}_{-9}	††	3055.9 ± 0.4 (*)	$156.6^{+79.5}_{-79.4}$	7.8 ± 1.9 (*)
$ l_\lambda=0, l_\rho=1, k_\lambda=0, k_\rho=0\rangle$	${}^2P_{3/2}$	3067^{+10}_{-10}	††	3078.6 ± 2.8 (*)	$99.9^{+47.4}_{-48.1}$	4.6 ± 3.3 (*)
$N = 2$						
$ l_\lambda=2, l_\rho=0, k_\lambda=0, k_\rho=0\rangle$	${}^2D_{3/2}$	3223^{+14}_{-14}	3218^{+17}_{-17}	†	$20.4^{+9.9}_{-10.0}$	†
$ l_\lambda=2, l_\rho=0, k_\lambda=0, k_\rho=0\rangle$	${}^2D_{5/2}$	3268^{+16}_{-16}	3261^{+21}_{-20}	†	$64.5^{+32.5}_{-33.2}$	†
$ l_\lambda=2, l_\rho=0, k_\lambda=0, k_\rho=0\rangle$	${}^4D_{1/2}$	3238^{+25}_{-25}	3239^{+23}_{-24}	†	$29.1^{+15.1}_{-15.4}$	†
$ l_\lambda=2, l_\rho=0, k_\lambda=0, k_\rho=0\rangle$	${}^4D_{3/2}$	3265^{+19}_{-19}	3265^{+18}_{-18}	†	$53.0^{+26.3}_{-26.6}$	†
$ l_\lambda=2, l_\rho=0, k_\lambda=0, k_\rho=0\rangle$	${}^4D_{5/2}$	3310^{+13}_{-13}	3308^{+15}_{-14}	†	$97.1^{+46.8}_{-47.6}$	†
$ l_\lambda=2, l_\rho=0, k_\lambda=0, k_\rho=0\rangle$	${}^4D_{7/2}$	3373^{+23}_{-23}	3368^{+25}_{-25}	†	$160.5^{+80.0}_{-80.2}$	†
$ l_\lambda=0, l_\rho=0, k_\lambda=1, k_\rho=0\rangle$	${}^2S_{1/2}$	3250^{+13}_{-14}	3244^{+18}_{-18}	†	$2.4^{+1.2}_{-1.2}$	†
$ l_\lambda=0, l_\rho=0, k_\lambda=1, k_\rho=0\rangle$	${}^4S_{3/2}$	3319^{+14}_{-14}	3316^{+15}_{-15}	†	$4.5^{+2.2}_{-2.3}$	†
$ l_\lambda=0, l_\rho=0, k_\lambda=0, k_\rho=1\rangle$	${}^2S_{1/2}$	3544^{+19}_{-19}	††	†	$20.6^{+10.3}_{-10.1}$	†
$ l_\lambda=0, l_\rho=0, k_\lambda=0, k_\rho=1\rangle$	${}^4S_{3/2}$	3613^{+20}_{-21}	††	†	$29.2^{+14.1}_{-14.4}$	†
$ l_\lambda=1, l_\rho=1, k_\lambda=0, k_\rho=0\rangle$	${}^2D_{3/2}$	3370^{+15}_{-15}	††	†	$228.5^{+111.9}_{-111.5}$	†
$ l_\lambda=1, l_\rho=1, k_\lambda=0, k_\rho=0\rangle$	${}^2D_{5/2}$	3415^{+17}_{-17}	††	†	$134.0^{+67.3}_{-66.4}$	†
$ l_\lambda=1, l_\rho=1, k_\lambda=0, k_\rho=0\rangle$	${}^2P_{1/2}$	3379^{+14}_{-14}	††	†	$2.5^{+1.2}_{-1.3}$	†
$ l_\lambda=1, l_\rho=1, k_\lambda=0, k_\rho=0\rangle$	${}^2P_{3/2}$	3406^{+16}_{-16}	††	†	$3.1^{+1.5}_{-1.5}$	†
$ l_\lambda=1, l_\rho=1, k_\lambda=0, k_\rho=0\rangle$	${}^2S_{1/2}$	3397^{+15}_{-15}	††	†	$56.4^{+28.2}_{-28.3}$	†
$ l_\lambda=0, l_\rho=2, k_\lambda=0, k_\rho=0\rangle$	${}^2D_{3/2}$	3517^{+19}_{-18}	††	†	$319.7^{+153.1}_{-157.5}$	†
$ l_\lambda=0, l_\rho=2, k_\lambda=0, k_\rho=0\rangle$	${}^2D_{5/2}$	3563^{+21}_{-21}	††	†	$232.2^{+115.8}_{-114.9}$	†
$ l_\lambda=0, l_\rho=2, k_\lambda=0, k_\rho=0\rangle$	${}^4D_{1/2}$	3532^{+29}_{-29}	††	†	$631.7^{+331.9}_{-330.5}$	†
$ l_\lambda=0, l_\rho=2, k_\lambda=0, k_\rho=0\rangle$	${}^4D_{3/2}$	3559^{+23}_{-23}	††	†	$452.4^{+221.5}_{-222.7}$	†
$ l_\lambda=0, l_\rho=2, k_\lambda=0, k_\rho=0\rangle$	${}^4D_{5/2}$	3604^{+20}_{-20}	††	†	$207.9^{+99.0}_{-99.0}$	†
$ l_\lambda=0, l_\rho=2, k_\lambda=0, k_\rho=0\rangle$	${}^4D_{7/2}$	3668^{+28}_{-28}	††	†	$578.0^{+293.4}_{-297.0}$	†

TABLE VI: As Table IV, but for $\Xi'_c(snc)$ resonances.

our theoretical mass is in good agreement with the experimental data, and the decay width is well reproduced. $\Sigma_c(2800)$ is identified as the first P_λ -wave excitation, with the assignment $J^P = 1/2^-$; the theoretical mass and width are compatible with the experimental data.

3. Ξ'_c and Ξ_c

Our results for Ξ'_c resonances are reported in Table VI and those for Ξ_c are reported in Table VII. The Ξ'_c states belong to the sextet configuration and the Ξ_c states belong to the anti- $\mathbf{3}$ -plet. Identifying the available data for

these states is more complex, since there are several theoretical excited states for Ξ'_c and Ξ_c in the same energy region. Additionally, for these states some experimental data are puzzling, as Ref. [3] reports a state with a central mass close to 2965 MeV. Hence, further studies are required in order to establish whether this narrow resonance is a different baryon from the narrow resonance at 2970 MeV found by Belle [6]. Moreover, the Belle collaboration recently measured the quantum numbers of $\Xi_c^+(2970)$ to be $J^P = 1/2^+$ [11], which could indicate a radial excitation. The observed masses of the ground states Ξ'_c and Ξ_c are well reproduced in our model, and are identified as $J^P = 1/2^+$ of the sextet and anti- $\mathbf{3}$ -plet,

$\Xi_c(snc)$ $\mathcal{F} = \mathbf{3}_c$	$2^{S+1}L_J$	Three-quark		Quark-diquark		
		Predicted Mass (MeV)	Predicted Mass (MeV)	Experimental Mass (MeV)	Predicted Γ_{tot} (MeV)	Experimental Γ (MeV)
$N = 0$						
$ l_\lambda=0, l_\rho=0, k_\lambda=0, k_\rho=0\rangle$	${}^2S_{1/2}$	2466^{+10}_{-10}	2473^{+10}_{-10}	2469.42 ± 1.77 (*)	$0.0^{+0.0}_{-0.0}$	≈ 0
$N = 1$						
$ l_\lambda=1, l_\rho=0, k_\lambda=0, k_\rho=0\rangle$	${}^2P_{1/2}$	2788^{+10}_{-10}	2789^{+9}_{-9}	2793.3 ± 0.28 (*)	$2.6^{+2.3}_{-2.1}$	9.5 ± 2.0 (*)
$ l_\lambda=1, l_\rho=0, k_\lambda=0, k_\rho=0\rangle$	${}^2P_{3/2}$	2815^{+10}_{-10}	2814^{+9}_{-9}	2818.49 ± 2.07 (*)	$4.6^{+2.2}_{-2.3}$	2.48 ± 0.5 (*)
$ l_\lambda=0, l_\rho=1, k_\lambda=0, k_\rho=0\rangle$	${}^2P_{1/2}$	2935^{+12}_{-12}	††	†	$17.0^{+8.6}_{-8.3}$	†
$ l_\lambda=0, l_\rho=1, k_\lambda=0, k_\rho=0\rangle$	${}^4P_{1/2}$	2977^{+20}_{-20}	††	2968.6 ± 3.3	$13.0^{+6.4}_{-6.4}$	20 ± 3.5
$ l_\lambda=0, l_\rho=1, k_\lambda=0, k_\rho=0\rangle$	${}^2P_{3/2}$	2962^{+12}_{-12}	††	†	$89.1^{+45.0}_{-45.0}$	†
$ l_\lambda=0, l_\rho=1, k_\lambda=0, k_\rho=0\rangle$	${}^4P_{3/2}$	3004^{+17}_{-17}	††	†	$56.2^{+29.7}_{-31.2}$	†
$ l_\lambda=0, l_\rho=1, k_\lambda=0, k_\rho=0\rangle$	${}^4P_{5/2}$	3049^{+18}_{-19}	††	†	$122.2^{+58.9}_{-59.6}$	†
$N = 2$						
$ l_\lambda=2, l_\rho=0, k_\lambda=0, k_\rho=0\rangle$	${}^2D_{3/2}$	3118^{+14}_{-14}	3113^{+14}_{-14}	3122.9 ± 1.23	$50.4^{+24.5}_{-24.6}$	4 ± 4
$ l_\lambda=2, l_\rho=0, k_\lambda=0, k_\rho=0\rangle$	${}^2D_{5/2}$	3164^{+16}_{-16}	3156^{+16}_{-16}	†	$131.8^{+62.8}_{-64.3}$	†
$ l_\lambda=0, l_\rho=0, k_\lambda=1, k_\rho=0\rangle$	${}^2S_{1/2}$	3145^{+14}_{-13}	3139^{+13}_{-14}	†	$5.1^{+2.5}_{-2.5}$	†
$ l_\lambda=0, l_\rho=0, k_\lambda=0, k_\rho=1\rangle$	${}^2S_{1/2}$	3440^{+20}_{-20}	††	†	$6.9^{+3.4}_{-3.4}$	†
$ l_\lambda=1, l_\rho=1, k_\lambda=0, k_\rho=0\rangle$	${}^2D_{3/2}$	3265^{+16}_{-16}	††	†	$53.9^{+26.3}_{-26.5}$	†
$ l_\lambda=1, l_\rho=1, k_\lambda=0, k_\rho=0\rangle$	${}^2D_{5/2}$	3311^{+17}_{-18}	††	†	$118.8^{+56.9}_{-57.6}$	†
$ l_\lambda=1, l_\rho=1, k_\lambda=0, k_\rho=0\rangle$	${}^4D_{1/2}$	3280^{+29}_{-29}	††	†	$23.5^{+11.6}_{-11.8}$	†
$ l_\lambda=1, l_\rho=1, k_\lambda=0, k_\rho=0\rangle$	${}^4D_{3/2}$	3307^{+23}_{-23}	††	†	$91.8^{+45.7}_{-45.6}$	†
$ l_\lambda=1, l_\rho=1, k_\lambda=0, k_\rho=0\rangle$	${}^4D_{5/2}$	3353^{+19}_{-19}	††	†	$152.8^{+75.3}_{-75.0}$	†
$ l_\lambda=1, l_\rho=1, k_\lambda=0, k_\rho=0\rangle$	${}^4D_{7/2}$	3416^{+26}_{-27}	††	†	$194.0^{+96.9}_{-96.0}$	†
$ l_\lambda=1, l_\rho=1, k_\lambda=0, k_\rho=0\rangle$	${}^2P_{1/2}$	3274^{+15}_{-15}	††	†	$0.4^{+0.2}_{-0.2}$	†
$ l_\lambda=1, l_\rho=1, k_\lambda=0, k_\rho=0\rangle$	${}^2P_{3/2}$	3302^{+16}_{-16}	††	†	$2.1^{+1.0}_{-1.0}$	†
$ l_\lambda=1, l_\rho=1, k_\lambda=0, k_\rho=0\rangle$	${}^4P_{1/2}$	3316^{+22}_{-22}	††	†	$0.3^{+0.1}_{-0.1}$	†
$ l_\lambda=1, l_\rho=1, k_\lambda=0, k_\rho=0\rangle$	${}^4P_{3/2}$	3344^{+19}_{-19}	††	†	$1.4^{+0.7}_{-0.7}$	†
$ l_\lambda=1, l_\rho=1, k_\lambda=0, k_\rho=0\rangle$	${}^4P_{5/2}$	3389^{+21}_{-22}	††	†	$3.7^{+1.9}_{-1.9}$	†
$ l_\lambda=1, l_\rho=1, k_\lambda=0, k_\rho=0\rangle$	${}^4S_{3/2}$	3362^{+19}_{-19}	††	†	$36.2^{+18.1}_{-17.9}$	†
$ l_\lambda=1, l_\rho=1, k_\lambda=0, k_\rho=0\rangle$	${}^2S_{1/2}$	3293^{+15}_{-15}	††	†	$29.9^{+14.8}_{-14.8}$	†
$ l_\lambda=0, l_\rho=2, k_\lambda=0, k_\rho=0\rangle$	${}^2D_{3/2}$	3413^{+20}_{-20}	††	†	$133.3^{+63.6}_{-64.0}$	†
$ l_\lambda=0, l_\rho=2, k_\lambda=0, k_\rho=0\rangle$	${}^2D_{5/2}$	3458^{+22}_{-22}	††	†	$118.5^{+59.0}_{-58.5}$	†

TABLE VII: As Table IV, but for $\Xi_c(snc)$ resonances.

respectively. $\Xi_c(2645)$ is identified as the $J^P = 3/2^+$ member of the sextet. In our model its mass is well reproduced and the width is underestimated. The states $\Xi_c(2790)$ and $\Xi_c(2815)$ are identified as $J^P = 1/2^-$ and $J^P = 3/2^-$ respectively, see Table VII; these quantum numbers, which have not yet been measured, refer to the first orbital excitations of the anti- $\mathbf{3}$ -plet states. $\Xi_c(2923)$ is identified as the P_λ -wave excitation $J^P = 1/2^-$ with spin $S = 3/2$ that belongs to the sextet; the theoretical width is compatible with the experimental value. Our assignment of $\Xi_c(2930)$ is to the P_λ -wave $J^P = 3/2^-$ state with $S = 1/2$ that belongs to the sextet; our theoretical mass deviates by 5 MeV, but our theoretical width is in good agreement with the experimental value. Moreover, there is another possible assignment, as the $J^P = 1/2^-$ state with $S = 1/2$ is close in mass, and belongs to the anti- $\mathbf{3}$ -plet; only future experiments will determine the

correct assignment.

Furthermore, there is a puzzle regarding the state observed by LHCb [3]: it has not been established whether the $\Xi_c^0(2965)$ state is the isospin partner of $\Xi_c^+(2970)$, or a different state. The complexity of identifying $\Xi_c(2965)$ is revealed by the fact that our model predicts two states, which adapt equally well for this state. The first $\Xi_c(2965)$ assignment is $J^P = 3/2^-$ with $S = 3/2$; this belongs to the sextet, and refers to a P_λ -wave excitation. The experimental mass and the width are well reproduced. A second identification of $\Xi_c(2965)$ is a P_ρ -wave $J^P = 1/2^-$ state with $S = 3/2$; thus, $\Xi_c(2965)$ would belong to the anti- $\mathbf{3}$ -plet, since we obtain a similar mass of 2978 ± 6 MeV and width that is compatible with the experimental value. It is noteworthy that, if the experiments confirm that there is a Ξ_c state at 2965 MeV which it is not a Roper state, it would mean that we could iden-

$\Lambda_c(nnc)$		Three-quark Quark-diquark				
$\mathcal{F} = \mathbf{3}_c$	$^{2S+1}L_J$	Predicted Mass (MeV)	Predicted Mass (MeV)	Experimental Mass (MeV)	Predicted Γ_{tot} (MeV)	Experimental Γ (MeV)
$N = 0$						
$ l_\lambda=0, l_\rho=0, k_\lambda=0, k_\rho=0\rangle$	$^2S_{1/2}$	2261^{+11}_{-11}	2264^{+10}_{-10}	2286.5 ± 0.14 (*)	$0.0^{+0.0}_{-0.0}$	≈ 0
$N = 1$						
$ l_\lambda=1, l_\rho=0, k_\lambda=0, k_\rho=0\rangle$	$^2P_{1/2}$	2616^{+10}_{-10}	2611^{+9}_{-9}	2592.3 ± 0.28 (*)	$1.4^{+0.8}_{-0.7}$	2.6 ± 0.6 (*)
$ l_\lambda=1, l_\rho=0, k_\lambda=0, k_\rho=0\rangle$	$^2P_{3/2}$	2643^{+10}_{-10}	2636^{+9}_{-9}	2625.0 ± 0.18 (*)	$9.8^{+4.8}_{-4.9}$	< 0.97
$ l_\lambda=0, l_\rho=1, k_\lambda=0, k_\rho=0\rangle$	$^2P_{1/2}$	2799^{+15}_{-15}	††	†	$56.9^{+27.4}_{-27.5}$	†
$ l_\lambda=0, l_\rho=1, k_\lambda=0, k_\rho=0\rangle$	$^4P_{1/2}$	2841^{+23}_{-23}	††	†	$32.5^{+15.6}_{-15.9}$	†
$ l_\lambda=0, l_\rho=1, k_\lambda=0, k_\rho=0\rangle$	$^2P_{3/2}$	2826^{+15}_{-15}	††	†	$92.7^{+45.1}_{-45.6}$	†
$ l_\lambda=0, l_\rho=1, k_\lambda=0, k_\rho=0\rangle$	$^4P_{3/2}$	2868^{+20}_{-20}	††	†	$121.9^{+58.9}_{-59.0}$	†
$ l_\lambda=0, l_\rho=1, k_\lambda=0, k_\rho=0\rangle$	$^4P_{5/2}$	2913^{+21}_{-21}	††	†	$108.0^{+52.4}_{-52.7}$	†
$N = 2$						
$ l_\lambda=2, l_\rho=0, k_\lambda=0, k_\rho=0\rangle$	$^2D_{3/2}$	2980^{+14}_{-14}	2967^{+14}_{-14}	2856.1 ± 6	$69.6^{+34.4}_{-34.1}$	68 ± 22
$ l_\lambda=2, l_\rho=0, k_\lambda=0, k_\rho=0\rangle$	$^2D_{5/2}$	3025^{+15}_{-15}	3009^{+16}_{-16}	2881.63 ± 0.24	$171.1^{+83.8}_{-82.8}$	5.6 ± 0.8
$ l_\lambda=0, l_\rho=0, k_\lambda=1, k_\rho=0\rangle$	$^2S_{1/2}$	3007^{+13}_{-13}	2992^{+14}_{-14}	2766 ± 2.4	$5.3^{+2.6}_{-2.6}$	50
$ l_\lambda=0, l_\rho=0, k_\lambda=0, k_\rho=1\rangle$	$^2S_{1/2}$	3372^{+29}_{-29}	††	†	$6.2^{+3.1}_{-3.1}$	†
$ l_\lambda=1, l_\rho=1, k_\lambda=0, k_\rho=0\rangle$	$^2D_{3/2}$	3163^{+20}_{-20}	††	†	$70.3^{+34.0}_{-34.2}$	†
$ l_\lambda=1, l_\rho=1, k_\lambda=0, k_\rho=0\rangle$	$^2D_{5/2}$	3208^{+21}_{-21}	††	†	$133.1^{+64.6}_{-64.9}$	†
$ l_\lambda=1, l_\rho=1, k_\lambda=0, k_\rho=0\rangle$	$^4D_{1/2}$	3178^{+33}_{-32}	††	†	$34.3^{+16.6}_{-16.6}$	†
$ l_\lambda=1, l_\rho=1, k_\lambda=0, k_\rho=0\rangle$	$^4D_{3/2}$	3205^{+28}_{-27}	††	†	$106.1^{+50.2}_{-52.0}$	†
$ l_\lambda=1, l_\rho=1, k_\lambda=0, k_\rho=0\rangle$	$^4D_{5/2}$	3250^{+24}_{-24}	††	†	$162.7^{+79.8}_{-78.7}$	†
$ l_\lambda=1, l_\rho=1, k_\lambda=0, k_\rho=0\rangle$	$^4D_{7/2}$	3313^{+30}_{-30}	††	†	$230.1^{+118.4}_{-116.4}$	†
$ l_\lambda=1, l_\rho=1, k_\lambda=0, k_\rho=0\rangle$	$^2P_{1/2}$	3172^{+20}_{-20}	††	†	$0.5^{+0.3}_{-0.3}$	†
$ l_\lambda=1, l_\rho=1, k_\lambda=0, k_\rho=0\rangle$	$^2P_{3/2}$	3199^{+20}_{-20}	††	†	$1.9^{+0.9}_{-0.9}$	†
$ l_\lambda=1, l_\rho=1, k_\lambda=0, k_\rho=0\rangle$	$^4P_{1/2}$	3214^{+26}_{-26}	††	†	$0.3^{+0.2}_{-0.2}$	†
$ l_\lambda=1, l_\rho=1, k_\lambda=0, k_\rho=0\rangle$	$^4P_{3/2}$	3241^{+24}_{-24}	††	†	$1.5^{+0.7}_{-0.7}$	†
$ l_\lambda=1, l_\rho=1, k_\lambda=0, k_\rho=0\rangle$	$^4P_{5/2}$	3286^{+26}_{-26}	††	†	$3.3^{+1.6}_{-1.7}$	†
$ l_\lambda=1, l_\rho=1, k_\lambda=0, k_\rho=0\rangle$	$^4S_{3/2}$	3259^{+24}_{-24}	††	†	$32.3^{+16.0}_{-16.4}$	†
$ l_\lambda=1, l_\rho=1, k_\lambda=0, k_\rho=0\rangle$	$^2S_{1/2}$	3190^{+20}_{-20}	††	†	$30.2^{+14.9}_{-15.1}$	†
$ l_\lambda=0, l_\rho=2, k_\lambda=0, k_\rho=0\rangle$	$^2D_{3/2}$	3345^{+30}_{-30}	††	†	$153.6^{+74.9}_{-74.4}$	†
$ l_\lambda=0, l_\rho=2, k_\lambda=0, k_\rho=0\rangle$	$^2D_{5/2}$	3390^{+30}_{-30}	††	†	$201.8^{+102.2}_{-101.6}$	†

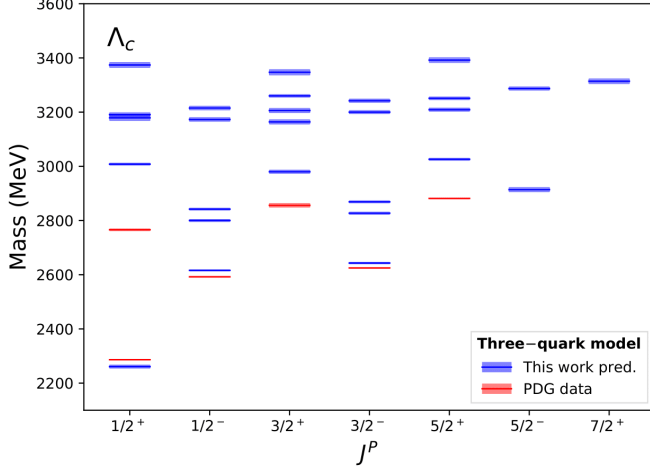
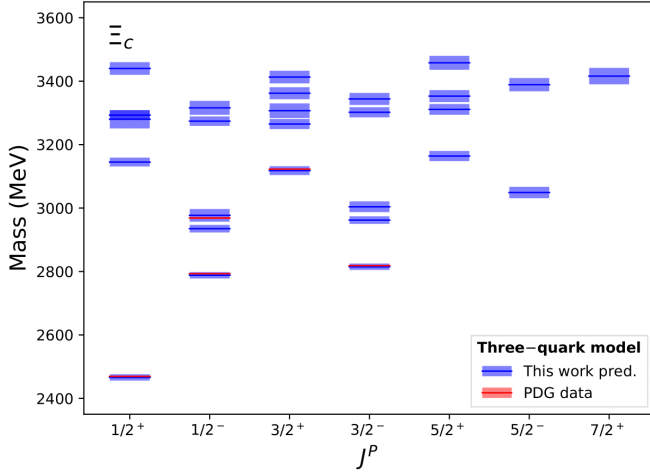
TABLE VIII: As Table IV, but for $\Lambda_c(nnc)$ resonances.

tify this state as a member of the sextet or anti- $\mathbf{3}$ -plet: either as a P_λ -wave excitation or as a P_ρ -wave excitation. The latter would imply that the charmed baryons behave as three-quark systems, instead of quark-diquark systems. Future experiments will help disentangle this puzzle. There is a similar situation for $\Xi_c(3055)$, where we also have two possible assignments. The first one is its identification as the first P_ρ -wave state in the sextet, with $J^P = 1/2^-$ and $S = 1/2$. Our theoretical mass exhibits a deviation of only 6 MeV, but the width is overestimated. The other possible $\Xi_c(3055)$ assignment is to the P_ρ -wave state in the anti- $\mathbf{3}$ -plet, with $J^P = 5/2^-$ and $S = 3/2$. Here, the mass is well reproduced and the width is overestimated. $\Xi_c(3080)$ is identified as the P_ρ -wave of the sextet, with $J^P = 1/2^-$ and $S = 3/2$. While our theoretical mass is well reproduced, our width is overestimated. Finally, $\Xi_c(3123)$ is identified as the first D_λ -wave exci-

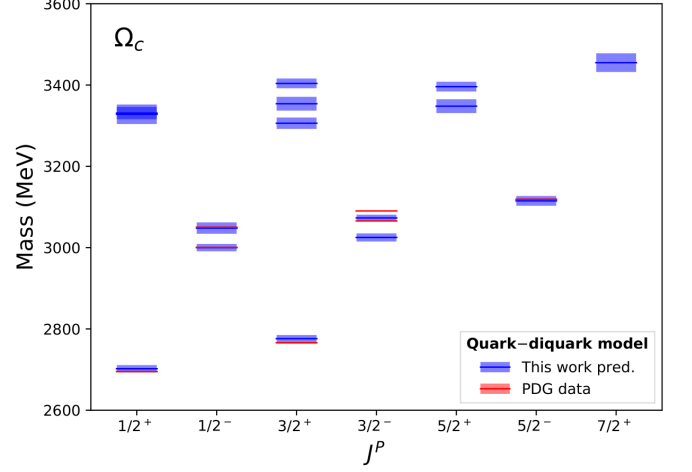
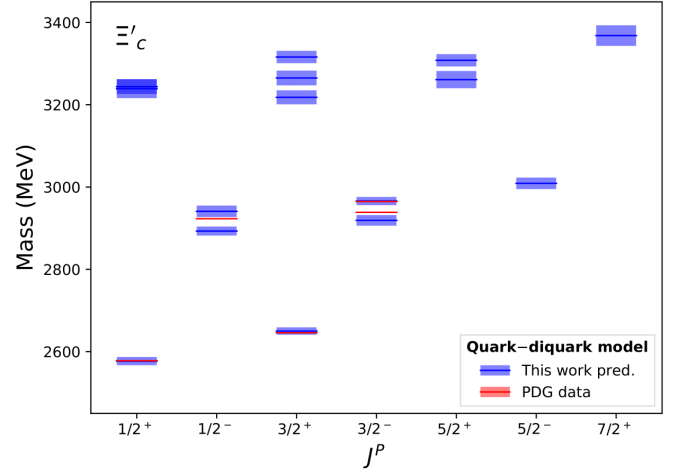
tation $J^P = 3/2^+$ with $S = 1/2$ of the anti- $\mathbf{3}$ -plet. The mass is well reproduced in our model but the width is overestimated.

4. Λ_c

Our results for Λ_c baryons are reported in Table VIII. The Λ_c^+ is identified as the ground state $J^P = 1/2^+$, with $S = 1/2$; its mass is well reproduced, with a small deviation of 15 MeV. For the excited states, we can observe a systematic deviation that exhibits the failure of the h.o. potential for these states. Nevertheless, the patterns in the theoretical mass spectrum can describe the experimental one. $\Lambda_c(2595)^+$ and $\Lambda_c(2625)^+$ are identified as our two P_λ -wave excitations $J^P = 1/2^-$ and $J^P = 3/2^-$, respectively, both with $S = 1/2$; their

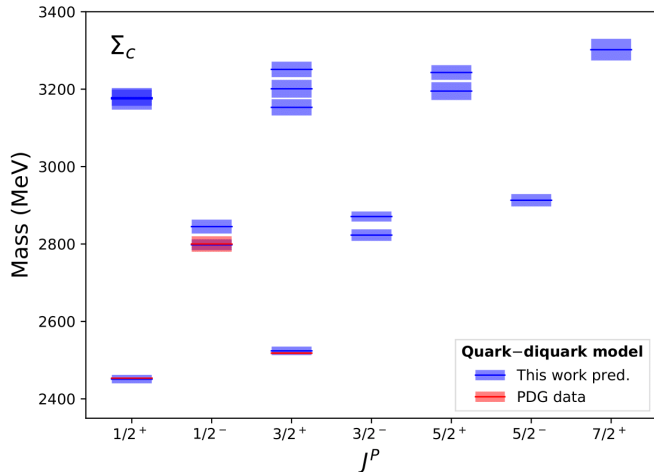
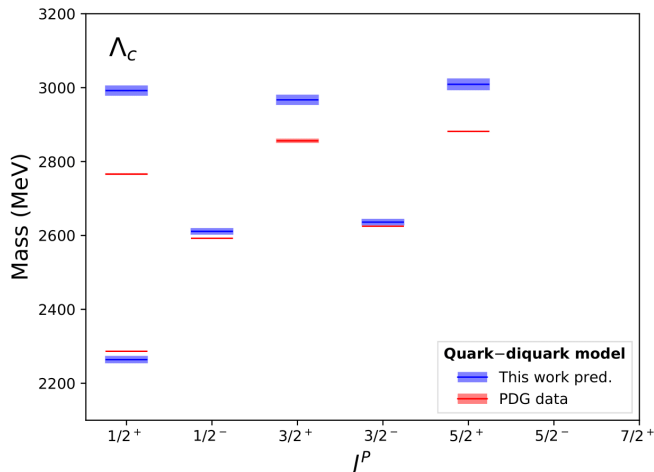
FIG. 5: As Figure 2, but for Λ_c resonances.FIG. 6: As Figure 2, but for Ξ_c resonances.

masses are reproduced with a deviation of 15 MeV. The theoretical width is compatible with the experimental for $\Lambda_c(2595)^+$ states value but overestimated for $\Lambda_c(2625)^+$. If the $\Lambda_c(2765)^+$ or $\Sigma_c(2765)$ state is identified as the Λ_c state in our model, there is no resonance within this energy region. Although it is close in energy to our predicted state $\Lambda_c(2800)^+$, $\Lambda_c(2765)^+$ is expected to be a Roper-like resonance. Consequently, we fail to reproduce the $\Lambda_c(2765)^+$ mass in our model, since our first theoretical radial excitation is the $\Lambda_c(3007)^+$ state. The observed $\Lambda_c(2860)^+$ is identified with our state $3/2^+$, having a significant predicted mass deviation of 100 MeV, but the theoretical decay width is well reproduced. Finally, the observed $\Lambda_c(2880)^+$ is identified with our state $5/2^+$. In this case, we also have a predicted mass with a deviation of 100 MeV, and a large deviation of the decay width.

FIG. 7: Ω_c mass spectra and tentative quantum number assignments on using the quark-diquark model. The theoretical predictions and their uncertainties (blue lines and bands) are compared with the experimental results (red lines and bands) reported in the PDG [9]. The experimental errors are too small to be evaluated on this energy scale.FIG. 8: As Figure 7, but for Ξ'_c resonances.

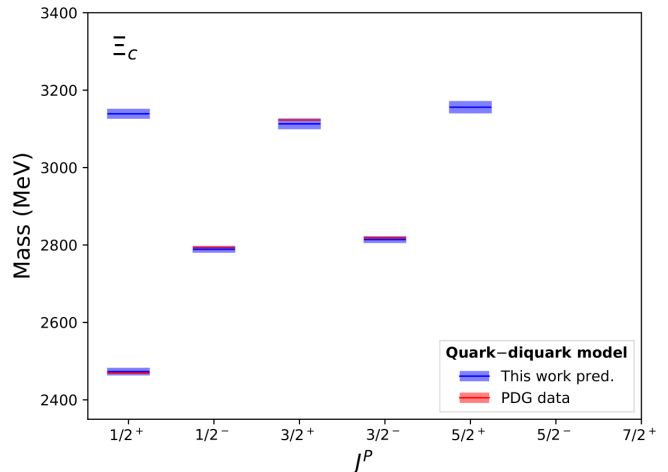
V. COMPARISON BETWEEN THE THREE-QUARK AND QUARK-DIQUARK STRUCTURES

In the light baryon sector, the successful constituent quark model reproduces the baryon mass spectra by assuming that the constituent quarks have roughly the same mass. This implies that the two oscillators, ρ - and λ , have the same frequency, $\omega_\rho \simeq \omega_\lambda$, meaning that the λ and ρ excitation states are degenerate in the mass spectrum. In the charm sector, we have a mass splitting between the λ and ρ , which comes from $\omega_\lambda - \omega_\rho \simeq 122$ MeV for Ω_c baryons, $\omega_\lambda - \omega_\rho \simeq 147$ MeV for Ξ_c and Ξ'_c

FIG. 9: As Figure 7, but for Σ_c resonances.FIG. 10: As Figure 7, but for Λ_c resonances.

baryons, and $\omega_\lambda - \omega_\rho \simeq 183$ MeV for Σ_c and Λ_c baryons. Consequently, we may expect to find these states in future experiments. However, given that the ρ states have not been observed, it seems that the charmed baryons can have a special internal structure which corresponds a quark-diquark configuration. The reduction of the effective degrees of freedom in the quark-diquark picture means fewer predicted states. We notice that, in the case of Λ_c and Ξ_c baryons, the number of states decreases drastically in the quark-diquark model, see Tables VIII and VII respectively. The lack of experimental data prevents us from reaching a decisive conclusion as to which description is better.

For instance, for the Ω_c baryons, we have identified all five P_λ -wave excited states, all with negative parity. We also expect two additional theoretical $\Omega_c(3129)$, $J = 1/2^-$ and $\Omega_c(3156)$, $J = 3/2^-$ states with negative par-

FIG. 11: As Figure 7, but for Ξ_c resonances.

ity. The existence of these states may indicate that the charmed baryons are not quark-diquark systems.

VI. CONCLUSIONS

We have calculated the mass spectra, strong partial decay widths and total decay widths of charmed baryons up to the D -wave shell for all the possible decay channels which respect quantum number conservation. All charmed baryons are simultaneously described by a global fit in which the same set of model parameters predicts the charm-baryon masses and strong partial decay widths in all the possible decay channels up to the D -wave shell. Moreover, the charm-baryon mass spectra are given in both the three-quark and the quark-diquark schemes. Propagation of the parameter uncertainties via a Monte Carlo bootstrap method is also included. This is often missing in theoretical papers on this subject. Nevertheless, it is necessary in order to guarantee a rigorous treatment of the uncertainties in the predicted mass spectra and decay widths. Our mass and strong partial decay width predictions are in good agreement with the available experimental data, and show the ability to guide future experimental searches by LHCb, Belle and Belle II. Moreover, for all the possible decay channels, we provide the flavor coupling coefficients, which are relevant to further theoretical investigations on charm-baryon strong decay widths. To the best of our knowledge, considering that the calculations of the strong decay widths are barely sensitive to the specific model used, our strong partial decay width predictions constitute the most complete calculation in the charm-baryon sector to date.

Acknowledgments

This work was supported in part by INFN, sezione di Genova. The authors acknowledge financial support from CONACyT, México (postdoctoral fellowship for H. García-Tecocoatzi); National Research Foundation of Korea (grants 2020R1I1A1A01066423, 2019R1I1A3A01058933, 2018R1A6A1A06024970 for A. Ramirez-Morales).

Appendix A: Baryon wave functions

1. The harmonic oscillator wave functions

In the heavy-light sector, the the ρ - and λ -modes decouple; therefore, they can be distinguished through an analysis of the heavy-light baryon mass spectra. This is because there is a difference in frequency between the ρ - and λ -modes,

$$\omega_\rho = \sqrt{\frac{3K_Q}{m_\rho}} \quad \text{and} \quad \omega_\lambda = \sqrt{\frac{3K_Q}{m_\lambda}}, \quad (\text{A1})$$

where m_ρ and m_λ are defined in Section II B . We write the baryon wave functions in terms of ω_ρ and ω_λ by using the relation $\alpha_{\rho,\lambda}^2 = \omega_{\rho,\lambda} m_{\rho,\lambda}$.

Also, we use the standard Jacobi coordinates:

$$\begin{aligned} \mathbf{p}_\rho &= \frac{1}{2}(\mathbf{p}_1 - \mathbf{p}_2) , \\ \mathbf{p}_\lambda &= \frac{1}{3}(\mathbf{p}_1 + \mathbf{p}_2 - 2\mathbf{p}_3) , \\ \mathbf{P}_{\text{cm}} &= \mathbf{p}_1 + \mathbf{p}_2 + \mathbf{p}_3 , \end{aligned} \quad (\text{A2})$$

for the baryon, and

$$\mathbf{q}_{\mathbf{c}} = \frac{1}{2}(\mathbf{p}_3 - \mathbf{p}_5) , \quad (\text{A3})$$

for the meson. In this coordinate system, \mathbf{p}_3 refers to the charm quark and $\mathbf{p}_{1,2}$ to the light quarks. Finally, \mathbf{p}_5 is the anti-quark momentum.

For the S -wave charmed baryon, we have,

$$\begin{aligned} \psi(0,0,0,0) &= 3^{3/4} \left(\frac{1}{\pi\omega_\rho m_\rho}\right)^{3/4} \left(\frac{1}{\pi\omega_\lambda m_\lambda}\right)^{3/4} \\ &\times \exp\left[-\frac{\mathbf{P}_\rho^2}{2\omega_\rho m_\rho} - \frac{\mathbf{P}_\lambda^2}{2\omega_\lambda m_\lambda}\right]. \end{aligned} \quad (\text{A4})$$

For the P -wave charmed baryon, we have,

$$\begin{aligned} \psi(1,m,0,0) &= -i 3^{3/4} \left(\frac{8}{3\sqrt{\pi}}\right)^{1/2} \left(\frac{1}{\omega_\rho m_\rho}\right)^{5/4} \mathcal{Y}_1^m(\mathbf{p}_\rho) \\ &\times \left(\frac{1}{\pi\omega_\lambda m_\lambda}\right)^{3/4} \exp\left[-\frac{\mathbf{P}_\rho^2}{2\omega_\rho m_\rho} - \frac{\mathbf{P}_\lambda^2}{2\omega_\lambda m_\lambda}\right], \end{aligned} \quad (\text{A5})$$

$$\begin{aligned} \psi(0,0,1,m) &= -i 3^{3/4} \left(\frac{8}{3\sqrt{\pi}}\right)^{1/2} \left(\frac{1}{\omega_\lambda m_\lambda}\right)^{5/4} \mathcal{Y}_1^m(\mathbf{p}_\lambda) \\ &\times \left(\frac{1}{\pi\omega_\rho m_\rho}\right)^{3/4} \exp\left[-\frac{\mathbf{P}_\rho^2}{2\omega_\rho m_\rho} - \frac{\mathbf{P}_\lambda^2}{2\omega_\lambda m_\lambda}\right]. \end{aligned} \quad (\text{A6})$$

For the D -wave charmed baryon, we have,

$$\begin{aligned} \psi(2,m,0,0) &= 3^{3/4} \left(\frac{16}{15\sqrt{\pi}}\right)^{1/2} \left(\frac{1}{\omega_\rho m_\rho}\right)^{7/4} \mathcal{Y}_2^m(\mathbf{p}_\rho) \\ &\times \left(\frac{1}{\pi\omega_\lambda m_\lambda}\right)^{3/4} \exp\left[-\frac{\mathbf{P}_\rho^2}{2\omega_\rho m_\rho} - \frac{\mathbf{P}_\lambda^2}{2\omega_\lambda m_\lambda}\right], \end{aligned} \quad (\text{A7})$$

$$\begin{aligned} \psi(0,0,2,m) &= 3^{3/4} \left(\frac{16}{15\sqrt{\pi}}\right)^{1/2} \left(\frac{1}{\omega_\lambda m_\lambda}\right)^{7/4} \mathcal{Y}_2^m(\mathbf{p}_\lambda) \\ &\times \left(\frac{1}{\pi\omega_\rho m_\rho}\right)^{3/4} \exp\left[-\frac{\mathbf{P}_\rho^2}{2\omega_\rho m_\rho} - \frac{\mathbf{P}_\lambda^2}{2\omega_\lambda m_\lambda}\right], \end{aligned} \quad (\text{A8})$$

$$\begin{aligned} \psi(1,m,1,m') &= -3^{3/4} \left(\frac{8}{3\sqrt{\pi}}\right)^{1/2} \left(\frac{1}{\omega_\rho m_\rho}\right)^{5/4} \mathcal{Y}_1^m(\mathbf{p}_\rho) \\ &\times \left(\frac{8}{3\sqrt{\pi}}\right)^{1/2} \left(\frac{1}{\omega_\lambda m_\lambda}\right)^{5/4} \mathcal{Y}_1^{m'}(\mathbf{p}_\lambda) \\ &\times \exp\left[-\frac{\mathbf{P}_\rho^2}{2\omega_\rho m_\rho} - \frac{\mathbf{P}_\lambda^2}{2\omega_\lambda m_\lambda}\right]. \end{aligned} \quad (\text{A9})$$

Here $\mathcal{Y}_l^m(\mathbf{p})$ is the solid harmonic polynomial. The wave function of the first radially excited charmed baryon $\psi(k_\lambda, k_\rho)$ reads as

$$\begin{aligned} \psi(1,0) &= 3^{3/4} \left(\frac{2}{3}\right)^{1/2} \left(\frac{1}{\pi^4\omega_\lambda m_\lambda \omega_\rho m_\rho}\right)^{3/4} \left[\frac{3}{2} - \frac{\mathbf{P}_\lambda^2}{\omega_\lambda m_\lambda}\right] \\ &\times \exp\left[-\frac{\mathbf{P}_\rho^2}{2\omega_\rho m_\rho} - \frac{\mathbf{P}_\lambda^2}{2\omega_\lambda m_\lambda}\right]. \end{aligned} \quad (\text{A10})$$

$$\begin{aligned} \psi(0,1) &= 3^{3/4} \left(\frac{2}{3}\right)^{1/2} \left(\frac{1}{\pi^4\omega_\lambda m_\lambda \omega_\rho m_\rho}\right)^{3/4} \left[\frac{3}{2} - \frac{\mathbf{P}_\rho^2}{\omega_\rho m_\rho}\right] \\ &\times \exp\left[-\frac{\mathbf{P}_\rho^2}{2\omega_\rho m_\rho} - \frac{\mathbf{P}_\lambda^2}{2\omega_\lambda m_\lambda}\right]. \end{aligned} \quad (\text{A11})$$

The ground state wave function of the meson is

$$\psi(0,0) = \left(\frac{R^2}{\pi}\right)^{3/4} \exp\left[-\frac{R^2(\mathbf{p}_3 - \mathbf{p}_5)^2}{8}\right]. \quad (\text{A12})$$

Appendix B: Flavor wave functions of charmed baryons

In the charm sector, we consider the **6-plet** and the $\bar{\mathbf{3}}$ -plet representation of the flavor wave functions. In the following subsections, we give the flavor wave functions of a charmed baryon A_c and its isospin quantum numbers $|A_c, I, M_I\rangle$.

a. 6-plet

$$|\Omega_c, 0, 0\rangle := |ssc\rangle \quad (\text{B1})$$

$$|\Xi_c^0, 1/2, -1/2\rangle := \frac{1}{\sqrt{2}}(|dsc\rangle + |sdc\rangle) \quad (\text{B2})$$

$$|\Xi_c^{'+}, 1/2, 1/2\rangle := \frac{1}{\sqrt{2}}(|usc\rangle + |suc\rangle) \quad (\text{B3})$$

$$|\Sigma_c^{++}, 1, 1\rangle := |uuc\rangle \quad (\text{B4})$$

$$|\Sigma_c^0, 1, -1\rangle := |ddc\rangle \quad (\text{B5})$$

$$|\Sigma_c^+, 1, 0\rangle := \frac{1}{\sqrt{2}}(|udc\rangle + |duc\rangle) \quad (\text{B6})$$

b. $\bar{\mathbf{3}}$ -plet

$$|\Xi_c^0, 1/2, -1/2\rangle := \frac{1}{\sqrt{2}}(|dsc\rangle - |sdc\rangle) \quad (\text{B7})$$

$$|\Xi_c^+, 1/2, 1/2\rangle := \frac{1}{\sqrt{2}}(|usc\rangle - |suc\rangle) \quad (\text{B8})$$

$$|\Lambda_c^+, 0, 0\rangle := \frac{1}{\sqrt{2}}(|udc\rangle - |duc\rangle) \quad (\text{B9})$$

Appendix C: Light-baryon wave functions

Whenever our final states contained a light baryon, we have used the following conventions, considering the S_3 invariant space-spin-flavor ($\Psi = \psi\chi\phi$). Thus, the light-baryon wave functions are given by

$$\begin{aligned} {}^2_8[56, L^P] &: \psi_S(\chi_\rho\phi_\rho + \chi_\lambda\phi_\lambda)/\sqrt{2}, \\ {}^2_8[70, L^P] &: [\psi_\rho(\chi_\rho\phi_\lambda + \chi_\lambda\phi_\rho) + \psi_\lambda(\chi_\rho\phi_\rho - \chi_\lambda\phi_\lambda)]/2, \\ {}^4_8[70, L^P] &: (\psi_\rho\phi_\rho + \psi_\lambda\phi_\lambda)\chi_S/\sqrt{2}, \\ {}^2_8[20, L^P] &: \psi_A(\chi_\rho\phi_\lambda - \chi_\lambda\phi_\rho)/\sqrt{2}, \\ {}^4_{10}[56, L^P] &: \psi_S\chi_S\phi_S, \\ {}^2_{10}[70, L^P] &: (\psi_\rho\chi_\rho + \psi_\lambda\chi_\lambda)\phi_S/\sqrt{2}, \\ {}^2_1[70, L^P] &: (\psi_\rho\chi_\lambda - \psi_\lambda\chi_\rho)\phi_A/\sqrt{2}, \\ {}^4_1[20, L^P] &: \psi_A\chi_S\phi_A. \end{aligned} \quad (\text{C1})$$

The quark orbital angular momentum \mathbf{L} is coupled with the spin \mathbf{S} to yield the total angular momentum \mathbf{J} of the baryon.

1. Flavor wave functions of light baryons

For the flavor wave functions $|(p, q), I, M_I, Y\rangle$ we adopt the convention of Ref. [69] with $(p, q) = (g_1 - g_2, g_2)$.

• The octet baryons

$$\begin{aligned} |(1, 1), \frac{1}{2}, \frac{1}{2}, 1\rangle &: \phi_\rho(p) = \frac{1}{\sqrt{2}}[|udu\rangle - |duu\rangle] \\ &: \phi_\lambda(p) = \frac{1}{\sqrt{6}}[2|uud\rangle - |udu\rangle \\ &\quad - |duu\rangle] \end{aligned} \quad (\text{C2})$$

$$\begin{aligned} |(1, 1), 1, 1, 0\rangle &: \phi_\rho(\Sigma^+) = \frac{1}{\sqrt{2}}[|suu\rangle - |usu\rangle] \\ &: \phi_\lambda(\Sigma^+) = \frac{1}{\sqrt{6}}[|suu\rangle + |usu\rangle \\ &\quad - 2|uus\rangle] \end{aligned} \quad (\text{C3})$$

$$\begin{aligned} |(1, 1), 0, 0, 0\rangle &: \phi_\rho(\Lambda) = \frac{1}{\sqrt{12}}[2|uds\rangle - 2|dus\rangle \\ &\quad - |dsu\rangle + |sdu\rangle \\ &\quad - |sud\rangle + |usd\rangle] \\ &: \phi_\lambda(\Lambda) = \frac{1}{2}[-|dsu\rangle - |sdu\rangle \\ &\quad + |sud\rangle + |usd\rangle] \end{aligned} \quad (\text{C4})$$

$$\begin{aligned} |(1, 1), \frac{1}{2}, \frac{1}{2}, -1\rangle &: \phi_\rho(\Xi^0) = \frac{1}{\sqrt{2}}[|sus\rangle - |uss\rangle] \\ &: \phi_\lambda(\Xi^0) = \frac{1}{\sqrt{6}}[2|ssu\rangle \\ &\quad - |sus\rangle - |uss\rangle] \end{aligned} \quad (\text{C5})$$

• The decuplet baryons

$$|(3, 0), \frac{3}{2}, \frac{3}{2}, 1\rangle : \phi_S(\Delta^{++}) = |uuu\rangle \quad (\text{C6})$$

$$|(3, 0), 1, 1, 0\rangle : \phi_S(\Sigma^+) = \frac{1}{\sqrt{3}}[|suu\rangle + |usu\rangle + |uus\rangle] \quad (\text{C7})$$

$$|(3, 0), \frac{1}{2}, \frac{1}{2}, -1\rangle : \phi_S(\Xi^0) = \frac{1}{\sqrt{3}}[|ssu\rangle + |sus\rangle + |uss\rangle] \quad (\text{C8})$$

$$|(3, 0), 0, 0, -2\rangle : \phi_S(\Omega^-) = |sss\rangle \quad (\text{C9})$$

• The singlet baryons

$$\begin{aligned} |(0, 0), 0, 0, 0\rangle &: \phi_A(\Lambda) = \frac{1}{\sqrt{6}}[|uds\rangle - |dus\rangle \\ &\quad + |dsu\rangle - |sdu\rangle \\ &\quad + |sud\rangle - |usd\rangle] \end{aligned} \quad (\text{C10})$$

Appendix D: Flavor wave functions of mesons

In the following subsections, we give the flavor wave functions of a meson C and its isospin quantum numbers $|C, I, M_I\rangle$.

1. Pseudoscalar mesons

Since the mixing angle $\theta_{\eta\eta'}$ between η and η' is small, we set $\theta_{\eta\eta'} = 0$. Thus, we identify $\eta = \eta_8$ and $\eta' = \eta_1$.

• The octet mesons

$$\begin{aligned}
|\pi^+, 1, 1\rangle &= -|u\bar{d}\rangle \\
|\pi^0, 1, 0\rangle &= \frac{1}{\sqrt{2}}[|u\bar{u}\rangle - |d\bar{d}\rangle] \\
|\pi^-, 1, -1\rangle &= |d\bar{u}\rangle \\
|K^+, 1/2, 1/2\rangle &= -|u\bar{s}\rangle \\
|K^-, 1/2, -1/2\rangle &= |s\bar{u}\rangle \\
|K^0, 1/2, -1/2\rangle &= -|d\bar{s}\rangle \\
|\bar{K}^0, 1/2, 1/2\rangle &= -|s\bar{d}\rangle \\
|\eta, 0, 0\rangle &= \frac{1}{\sqrt{6}}[|u\bar{u}\rangle + |d\bar{d}\rangle - 2|s\bar{s}\rangle]
\end{aligned} \tag{D1}$$

• The singlet mesons

$$|\eta', 0, 0\rangle = \frac{1}{\sqrt{3}}[|u\bar{u}\rangle + |d\bar{d}\rangle + |s\bar{s}\rangle] \tag{D2}$$

2. Vector Mesons

We consider that the ϕ meson is a pure $s\bar{s}$ state; thus, we have the following wave functions:

• The octet mesons

$$\begin{aligned}
|\rho^+, 1, 1\rangle &= -|u\bar{d}\rangle \\
|\rho^0, 1, 0\rangle &= \frac{1}{\sqrt{2}}[|u\bar{u}\rangle - |d\bar{d}\rangle] \\
|\rho^-, 1, -1\rangle &= |d\bar{u}\rangle \\
|K^{*+}, 1/2, 1/2\rangle &= -|u\bar{s}\rangle \\
|K^{*-}, 1/2, -1/2\rangle &= |s\bar{u}\rangle \\
|K^{*0}, 1/2, -1/2\rangle &= -|d\bar{s}\rangle \\
|\bar{K}^{*0}, 1/2, 1/2\rangle &= -|s\bar{d}\rangle \\
|\omega, 0, 0\rangle &= \frac{1}{\sqrt{2}}[|u\bar{u}\rangle + |d\bar{d}\rangle]
\end{aligned} \tag{D3}$$

• The singlet mesons

$$|\phi, 0, 0\rangle = |s\bar{s}\rangle \tag{D4}$$

3. Charmed Mesons

In the case of charmed- D mesons, the flavor wave functions are the same for the pseudoscalar and vector states. We use the following flavor wave functions:

$$\begin{aligned}
|D_s^{+*}, 0, 0\rangle &= |D_s^+, 0, 0\rangle = |c\bar{s}\rangle \\
|D_s^{+*}, 1/2, 1/2\rangle &= |D_s^+, 1/2, 1/2\rangle = |c\bar{d}\rangle \\
|D_s^{0*}, 1/2, -1/2\rangle &= |D_s^0, 1/2, -1/2\rangle = |c\bar{u}\rangle
\end{aligned}$$

Appendix E: Flavor coupling

In the following subsections, we give the flavor coefficients $\mathcal{F}_{A\rightarrow BC}$ used to calculate the transition amplitudes. We compute $\mathcal{F}_{A\rightarrow BC} = \langle\phi_B\phi_C|\phi_0\phi_A\rangle$ where $\phi_{(A,B,C)}$ refers to the initial flavor wave function of a charmed baryon ϕ_{A_c} , final baryon ϕ_B , and final meson ϕ_C , respectively; $\phi_0^{45} = (u\bar{u} + d\bar{d} + s\bar{s})/\sqrt{3}$ is the flavor singlet-wave function of $SU(3)$. In addition, we compute the flavor decay coefficients of the isospin channels, since we assume that the isospin symmetry holds even though it is slightly broken. The corresponding charge channels are obtained by multiplying our $\mathcal{F}_{A\rightarrow BC}$ by the corresponding Clebsch-Gordan coefficient in the isospin space, using the convention of the isospin quantum numbers of the baryons and meson flavor wave functions found in B, C 1, and D. Thus, the flavor charge channel for a specific projection (I, M_I) in the isospin channel is obtained as follows:

$$\begin{aligned}
&\mathcal{F}_{A(I_A, M_{I_A})\rightarrow B(I_B, M_{I_B})C(I_C, M_{I_C})} = \\
&\langle\phi_B, I_B, M_{I_B}, \phi_C, I_C, M_{I_C}|\phi_0, 0, 0, \phi_A, I_A, M_{I_A}\rangle_F \\
&= \langle I_B, M_{I_B}, I_C, M_{I_C}|I_A, M_{I_A}\rangle\mathcal{F}_{A\rightarrow BC}, \tag{E1}
\end{aligned}$$

where $\langle I_B, M_{I_B}, I_C, M_{I_C}|I_A, M_{I_A}\rangle$ is a Clebsch-Gordan coefficient and the flavor functions ϕ_i of each baryon and meson have a specific isospin projection M_I .

1. charmed baryons and pseudoscalar mesons

We give the squared flavor-coupling coefficients, $\mathcal{F}_{A\rightarrow BC}^2$, when the final states have a pseudoscalar light meson. Here, A and B are charmed baryons, and the subindexes $\mathbf{6}_f$ and $\mathbf{3}_f$ refer to the sextet and the anti-triplet baryon multiplets. The C is a pseudoscalar meson and the subindexes $\mathbf{8}$ and $\mathbf{1}$ refer to the octet and singlet meson multiplets, respectively.

$$\bullet A_{\mathbf{6}_f} \rightarrow B_{\mathbf{6}_f} + C_{\mathbf{8}}$$

$$\begin{aligned}
\begin{pmatrix} \Omega_c \\ \Sigma_c \\ \Xi'_c \end{pmatrix} &\rightarrow \begin{pmatrix} \Xi'_c K & \Omega_c \eta \\ \Xi'_c K & \Sigma_c \pi & \Sigma_c \eta \\ \Sigma_c K & \Xi'_c \pi & \Xi'_c \eta \end{pmatrix} \\
&= \begin{pmatrix} \frac{1}{3} & \frac{1}{3} \\ \frac{1}{6} & \frac{1}{3} & \frac{1}{18} \\ \frac{1}{4} & \frac{1}{8} & \frac{1}{72} \end{pmatrix}
\end{aligned} \tag{E2}$$

- $A_{\mathbf{6}_f} \rightarrow B_{\mathbf{6}_f} + C_1$

$$\begin{pmatrix} \Omega_c \\ \Sigma_c \\ \Xi'_c \end{pmatrix} \rightarrow \begin{pmatrix} \Omega_c \eta' \\ \Sigma_c \eta' \\ \Xi'_c \eta' \end{pmatrix} = \begin{pmatrix} \frac{1}{3} \\ \frac{1}{9} \\ \frac{1}{9} \end{pmatrix} \tag{E3}$$

- $A_{\mathbf{6}_f} \rightarrow B_{\mathbf{3}_f} + C_8$

$$\begin{aligned}
\begin{pmatrix} \Omega_c \\ \Sigma_c \\ \Xi'_c \end{pmatrix} &\rightarrow \begin{pmatrix} \Xi_c K \\ \Xi_c K & \Lambda_c \pi \\ \Lambda_c K & \Xi_c \pi & \Xi_c \eta \end{pmatrix} \\
&= \begin{pmatrix} \frac{1}{3} \\ \frac{1}{6} & \frac{1}{2} \\ \frac{1}{12} & \frac{1}{8} & \frac{1}{72} \end{pmatrix}
\end{aligned} \tag{E4}$$

- $A_{\mathbf{6}_f} \rightarrow B_{\mathbf{3}_f} + C_1$

$$(\Xi'_c) \rightarrow (\Xi_c \eta') = \left(\frac{1}{9} \right) \tag{E5}$$

- $A_{\mathbf{3}_f} \rightarrow B_{\mathbf{6}_f} + C_8$

$$\begin{aligned}
\begin{pmatrix} \Lambda_c \\ \Xi_c \end{pmatrix} &\rightarrow \begin{pmatrix} \Xi'_c K & \Sigma_c \pi \\ \Sigma_c K & \Xi'_c \pi & \Xi'_c \eta \end{pmatrix} \\
&= \begin{pmatrix} \frac{1}{6} & \frac{1}{2} \\ \frac{1}{4} & \frac{1}{8} & \frac{1}{72} \end{pmatrix}
\end{aligned} \tag{E6}$$

- $A_{\mathbf{3}_f} \rightarrow B_{\mathbf{6}_f} + C_1$

$$(\Xi_c) \rightarrow (\Xi'_c \eta') = \left(\frac{1}{9} \right) \tag{E7}$$

- $A_{\mathbf{3}_f} \rightarrow B_{\mathbf{3}_f} + C_8$

$$\begin{aligned}
\begin{pmatrix} \Lambda_c \\ \Xi_c \end{pmatrix} &\rightarrow \begin{pmatrix} \Xi_c K & \Lambda_c \eta \\ \Lambda_c K & \Xi_c \pi & \Xi_c \eta \end{pmatrix} \\
&= \begin{pmatrix} \frac{1}{6} & \frac{1}{18} \\ \frac{1}{12} & \frac{1}{8} & \frac{1}{72} \end{pmatrix}
\end{aligned} \tag{E8}$$

- $A_{\mathbf{3}_f} \rightarrow B_{\mathbf{3}_f} + C_1$

$$\begin{pmatrix} \Lambda_c \\ \Xi_c \end{pmatrix} \rightarrow \begin{pmatrix} \Lambda_c \eta' \\ \Xi_c \eta' \end{pmatrix} = \begin{pmatrix} \frac{1}{9} \\ \frac{1}{9} \end{pmatrix} \tag{E9}$$

2. Charmed baryons and vector mesons

We give the squared flavor-coupling coefficients, $\mathcal{F}_{A \rightarrow BC}^2$, when the final states have a vector-light meson. Here A and B are charmed baryons, and the subindexes $\mathbf{6}_f$ and $\mathbf{3}_f$ refer to the sextet and the anti-triplet baryon multiplets. The C is a vector meson and the subindexes $\mathbf{8}$ and $\mathbf{1}$ refer to the octet and singlet meson multiplets respectively.

- $A_{\mathbf{6}_f} \rightarrow B_{\mathbf{6}_f} + C_8$

$$\begin{aligned}
\begin{pmatrix} \Omega_c \\ \Sigma_c \\ \Xi'_c \end{pmatrix} &\rightarrow \begin{pmatrix} \Xi'_c K^* \\ \Xi'_c K^* & \Sigma_c \rho & \Sigma_c \omega \\ \Sigma_c K^* & \Xi'_c \rho & \Xi'_c \omega \end{pmatrix} \\
&= \begin{pmatrix} \frac{1}{3} \\ \frac{1}{6} & \frac{1}{3} & \frac{1}{6} \\ \frac{1}{4} & \frac{1}{8} & \frac{1}{24} \end{pmatrix}
\end{aligned} \tag{E10}$$

- $A_{\mathbf{6}_f} \rightarrow B_{\mathbf{6}_f} + C_1$

$$\begin{pmatrix} \Omega_c \\ \Sigma_c \\ \Xi'_c \end{pmatrix} \rightarrow \begin{pmatrix} \Omega_c \phi \\ \Sigma_c \phi \\ \Xi'_c \phi \end{pmatrix} = \begin{pmatrix} \frac{1}{9} \\ 0 \\ \frac{1}{2} \end{pmatrix} \tag{E11}$$

- $A_{\mathbf{6}_f} \rightarrow B_{\mathbf{3}_f} + C_{\mathbf{8}}$

$$\begin{aligned} \begin{pmatrix} \Omega_c \\ \Sigma_c \\ \Xi'_c \end{pmatrix} &\rightarrow \begin{pmatrix} & \Xi_c K^* \\ \Xi_c K^* & \Lambda_c \rho \\ \Lambda_c K^* & \Xi_c \rho & \Xi_c \omega \end{pmatrix} \\ &= \begin{pmatrix} \frac{1}{3} \\ \frac{1}{6} & \frac{1}{3} \\ \frac{1}{12} & \frac{1}{8} & \frac{1}{24} \end{pmatrix} \end{aligned} \quad (\text{E12})$$

- $A_{\mathbf{6}_f} \rightarrow B_{\mathbf{3}_f} + C_{\mathbf{1}}$

$$(\Xi'_c) \rightarrow (\Xi_c \phi) = \left(\frac{1}{12} \right) \quad (\text{E13})$$

- $A_{\mathbf{3}_f} \rightarrow B_{\mathbf{6}_f} + C_{\mathbf{8}}$

$$\begin{aligned} \begin{pmatrix} \Lambda_c \\ \Xi_c \end{pmatrix} &\rightarrow \begin{pmatrix} \Xi'_c K^* & \Sigma_c \rho \\ \Sigma_c K^* & \Xi'_c \rho & \Xi'_c \omega \end{pmatrix} \\ &= \begin{pmatrix} \frac{1}{6} & \frac{1}{2} \\ \frac{1}{4} & \frac{1}{8} & \frac{1}{24} \end{pmatrix} \end{aligned} \quad (\text{E14})$$

- $A_{\mathbf{3}_f} \rightarrow B_{\mathbf{6}_f} + C_{\mathbf{1}}$

$$(\Xi_c) \rightarrow (\Xi'_c \phi) = \left(\frac{1}{12} \right) \quad (\text{E15})$$

- $A_{\mathbf{3}_f} \rightarrow B_{\mathbf{3}_f} + C_{\mathbf{8}}$

$$\begin{aligned} \begin{pmatrix} \Lambda_c \\ \Xi_c \end{pmatrix} &\rightarrow \begin{pmatrix} \Xi_c K^* & \Lambda_c \omega \\ \Lambda_c K^* & \Xi_c \rho & \Xi_c \omega \end{pmatrix} \\ &= \begin{pmatrix} \frac{1}{6} & \frac{1}{6} \\ \frac{1}{12} & \frac{1}{8} & \frac{1}{24} \end{pmatrix} \end{aligned} \quad (\text{E16})$$

- $A_{\mathbf{3}_f} \rightarrow B_{\mathbf{3}_f} + C_{\mathbf{1}}$

$$\begin{pmatrix} \Lambda_c \\ \Xi_c \end{pmatrix} \rightarrow \begin{pmatrix} \Lambda_c \phi \\ \Xi_c \phi \end{pmatrix} = \begin{pmatrix} 0 \\ \frac{1}{12} \end{pmatrix} \quad (\text{E17})$$

3. Light baryons and charm-(pseudoscalar/vector) mesons

We give the $\mathcal{F}_{A \rightarrow BC}^2$ when the final states have a light baryon and a charm-(pseudoscalar/vector) meson. Since the mesons D^0 and D^+ form an isospin doublet, both are treated as D in the tables; whereas D_s is separated by the strangeness content. The subindexes $\mathbf{6}_f$ and $\mathbf{3}_f$ refer to the sextet and the anti-triplet baryon multiplets for the initial charmed baryon A , whereas the final B baryons can have subindexes $\mathbf{8}$ or $\mathbf{10}$, according to whether the final light baryon belongs to the octet or decuplet baryon multiplets. Additionally, owing to the symmetry of the wave functions of the octet-light baryons, see C1, we can have only ρ or λ contributions in the final states, as indicated by a superindex.

- $A_{\mathbf{6}_f} \rightarrow B_{\mathbf{10}} + C$

$$\begin{pmatrix} \Omega_c \\ \Sigma_c \\ \Xi'_c \end{pmatrix} \rightarrow \begin{pmatrix} \Xi_{10}^* D & \Omega_{10} D_s \\ \Delta D & \Sigma_{10}^* D_s \\ \Sigma_{10}^* D & \Xi_{10}^* D_s \end{pmatrix} = \begin{pmatrix} \frac{2}{9} & \frac{1}{3} \\ \frac{4}{9} & \frac{1}{9} \\ \frac{1}{3} & \frac{2}{9} \end{pmatrix} \quad (\text{E18})$$

- $A_{\mathbf{6}_f} \rightarrow B_{\mathbf{8}} + C$

$$\begin{pmatrix} \Omega_c \\ \Sigma_c \\ \Xi'_c \end{pmatrix} \rightarrow \begin{pmatrix} \Xi_8^\lambda D \\ N^\lambda D & \Sigma_8^\lambda D_s \\ \Sigma_8^\lambda D & \Xi_8^\lambda D_s \end{pmatrix} = \begin{pmatrix} \frac{4}{9} \\ \frac{2}{9} & \frac{2}{9} \\ \frac{1}{6} & \frac{1}{9} \end{pmatrix} \quad (\text{E19})$$

- $A_{\mathbf{3}_f} \rightarrow B_{\mathbf{8}} + C$

$$\begin{aligned} \begin{pmatrix} \Lambda_c \\ \Xi_c \end{pmatrix} &\rightarrow \begin{pmatrix} N^\rho D & \Lambda_8^\rho D_s \\ \Sigma_8^\rho D & \Xi_8^\rho D_s & \Lambda_8^\rho D \end{pmatrix} \\ &= \begin{pmatrix} \frac{2}{3} & \frac{2}{9} \\ \frac{1}{2} & \frac{1}{3} & \frac{1}{18} \end{pmatrix} \end{aligned} \quad (\text{E20})$$

Appendix F: Partial decay widths

The partial-decay widths, $\Gamma_{A \rightarrow BC}$, of an initial baryon A decaying to a final baryon B plus a meson C , in all the open-flavor channels, are shown in Tables IX-XIII. Here, we give the contribution of the isospin channels. The charge channel width for baryon A with isospin projection $|A, I, M_{I_A}\rangle$ can be obtain as follows

$$\begin{aligned} &\Gamma_{A(I_A, M_{I_A}) \rightarrow B(I_B, M_{I_B}) C(I_C, M_{I_C})} = \\ &\langle I_B, M_{I_B}, I_C, M_{I_C} | I_A, M_{I_A} \rangle^2 \Gamma_{A \rightarrow BC}, \end{aligned} \quad (\text{F1})$$

where $\langle I_B, M_{I_B}, I_C, M_{I_C} | I_A, M_{I_A} \rangle$ is a Clebsch-Gordan coefficient, and the partial decay width $\Gamma_{A \rightarrow BC}$ can be extracted from Tables IX-XIII.

State	$\Xi_c K$	$\Xi'_c K$	$\Xi_c^* K$	$\Xi_c K^*$	$\Xi'_c K^*$	$\Xi_c^* K^*$	$\Xi_c K^* \Omega_c \eta$	$\Omega_c^* \eta$	$\Omega_c \phi$	$\Omega_c^* \phi$	$\Omega_c \eta'$	$\Omega_c^* \eta'$	$\Xi_8 D$	$\Xi_{10} D$	Tot Γ
$^2S_{1/2}$	†	†	†	†	†	†	†	†	†	†	†	†	†	†	†
$^4S_{3/2}$	†	†	†	†	†	†	†	†	†	†	†	†	†	†	†
$^2P_{1/2}$	4.1	†	†	†	†	†	†	†	†	†	†	†	†	†	4.1
$^4P_{1/2}$	7.5	0.1	†	†	†	†	†	†	†	†	†	†	†	†	7.6
$^2P_{3/2}$	26.3	†	†	†	†	†	†	†	†	†	†	†	†	†	26.3
$^4P_{3/2}$	6.3	0.4	†	†	†	†	†	†	†	†	†	†	†	†	6.7
$^4P_{5/2}$	40.9	8.9	0.3	†	†	†	†	†	†	†	†	†	†	†	50.1
$^2P_{1/2}$	†	8.9	5.5	†	†	†	†	†	†	†	†	†	†	†	14.4
$^2P_{3/2}$	†	61.1	10.5	†	†	†	†	†	†	†	†	†	†	†	71.6
$^2D_{3/2}$	1.9	1.8	2.3	†	†	†	0.3	†	†	†	†	†	4.3	†	10.6
$^2D_{5/2}$	5.4	5.1	0.5	†	†	†	1.2	†	†	†	†	†	12.2	†	24.4
$^4D_{1/2}$	0.2	0.2	3.3	†	†	†	0.1	0.1	†	†	†	†	12.3	†	16.2
$^4D_{3/2}$	2.0	0.5	5.2	0.2	†	†	0.2	0.6	†	†	†	†	21.7	†	30.4
$^4D_{5/2}$	5.0	1.2	5.0	1.6	†	†	0.3	1.2	†	†	†	†	46.9	1.1	62.3
$^4D_{7/2}$	7.8	2.0	5.0	2.6	†	†	0.8	0.9	†	†	†	†	83.2	20.9	123.2
$^2S_{1/2}$	0.2	0.3	0.1	†	†	†	0.1	†	†	†	†	†	0.5	†	1.2
$^4S_{3/2}$	0.2	0.1	0.4	0.2	†	†	†	0.1	†	†	†	†	2.1	0.2	3.3
$^2S_{1/2}$	0.3	1.0	0.7	3.0	11.6	0.1	1.1	0.5	†	†	†	†	†	†	18.3
$^4S_{3/2}$	0.1	0.1	1.2	2.8	1.0	17.2	0.2	1.4	†	†	†	†	†	†	24.0
$^2D_{3/2}$	†	6.5	107.0	53.5	†	†	4.0	27.0	†	†	†	†	†	†	198.0
$^2D_{5/2}$	†	56.4	16.8	17.2	0.4	†	20.9	3.3	†	†	†	†	†	†	115.0
$^2P_{1/2}$	†	†	1.4	0.4	†	†	†	0.3	†	†	†	†	†	†	2.1
$^2P_{3/2}$	†	1.1	0.8	0.7	†	†	0.3	0.2	†	†	†	†	†	†	3.1
$^2S_{1/2}$	†	7.6	22.3	36.1	0.2	†	8.6	13.5	†	†	†	†	†	†	88.3
$^2D_{3/2}$	18.4	16.8	18.8	28.7	115.1	†	8.0	11.2	†	†	†	†	†	†	217.0
$^2D_{5/2}$	48.3	49.7	14.5	3.6	30.8	0.7	23.3	3.4	†	†	†	†	†	†	174.3
$^4D_{1/2}$	9.4	0.4	33.1	38.8	7.0	111.6	0.3	17.0	†	†	†	†	†	†	217.6
$^4D_{3/2}$	22.1	4.9	28.2	77.3	16.8	111.4	2.2	21.9	†	†	†	†	†	†	284.8
$^4D_{5/2}$	38.6	10.8	32.8	47.8	13.2	43.7	5.4	19.7	†	†	†	†	†	†	212.0
$^4D_{7/2}$	72.1	18.0	88.1	107.8	18.0	38.9	8.4	29.2	0.1	†	2.3	0.1	†	†	383.0

TABLE IX: Partial decay widths for $\Omega_c(ssc)$; the values are given in MeV. The partial decay widths are computed by means of Eq. 7. The states are labeled with the spectroscopic notation $^{2S+1}L_J$, which is characterized by total angular momentum $\mathbf{J} = \mathbf{L} + \mathbf{S}_{\text{tot}}$, where $\mathbf{S}_{\text{tot}} = \mathbf{S}_\rho + \frac{1}{2}$, and $L = \mathbf{l}_\rho + \mathbf{l}_\lambda$. The order of the states is the same as is presented in Table IV.

State	$\Sigma_c\pi$	$\Sigma_c^*\pi$	$\Lambda_c\pi$	$\Sigma_c\eta$	Ξ_cK	$\Sigma_c\rho$	$\Sigma_c^*\rho$	$\Lambda_c\rho$	$\Sigma_c^*\eta$	$\Sigma_c\eta'$	$\Sigma_c^*\eta'$	$\Xi_c'K'$	Ξ_c^*K'	Ξ_cK^*	$\Xi_c'K^*$	$\Xi_c^*K^*\Sigma\omega$	$\Sigma_c^*\omega$	ND	$\Sigma_8 D_8 ND^*$	ΔD	N_1^*D	N_2^*D	N_3^*D	N_4^*D	Tot Γ		
$^2S_{1/2}$	†	†	1.7	†	†	†	†	†	†	†	†	†	†	†	†	†	†	†	†	†	†	†	†	†	1.7		
$^4S_{3/2}$	†	†	14.9	†	†	†	†	†	†	†	†	†	†	†	†	†	†	†	†	†	†	†	†	†	†	14.9	
$^2P_{1/2}$	2.2	17.4	0.1	†	†	†	†	†	†	†	†	†	†	†	†	†	†	0.8	†	9.9	†	†	†	†	†	30.4	
$^4P_{1/2}$	0.7	9.9	1.7	†	†	†	†	†	†	†	†	†	†	†	†	†	†	13.3	†	35.6	†	†	†	†	†	61.2	
$^2P_{3/2}$	28.7	2.8	45.2	†	†	†	†	†	†	†	†	†	†	†	†	†	†	9.0	†	97.0	†	†	†	†	†	182.7	
$^4P_{3/2}$	1.6	39.0	9.8	†	†	†	†	†	†	†	†	†	†	†	†	†	†	9.8	†	104.9	†	†	†	†	†	165.1	
$^4P_{5/2}$	10.5	22.8	64.8	†	†	†	†	†	†	†	†	†	†	†	†	†	†	65.4	†	73.0	†	†	†	†	†	236.5	
$^2P_{1/2}$	0.5	123.8	†	0.3	†	†	†	†	†	†	†	†	†	†	†	†	†	†	†	†	†	†	†	†	†	124.6	
$^2P_{3/2}$	64.0	55.4	†	5.4	†	†	†	0.2	†	†	†	†	†	†	†	†	†	†	†	†	†	†	†	†	†	125.0	
$^2D_{3/2}$	2.5	3.3	4.9	0.3	0.7	†	†	4.3	0.3	†	†	0.4	0.2	†	†	†	†	3.8	1.4	55.9	77.0	†	†	†	†	155.0	
$^2D_{5/2}$	7.6	1.8	12.8	0.8	1.9	0.1	†	0.3	0.1	†	†	1.3	0.1	†	†	†	†	11.3	4.5	110.9	96.1	†	†	†	†	249.6	
$^4D_{1/2}$	†	5.4	2.4	†	0.3	†	†	5.5	0.4	†	†	0.1	0.4	†	†	†	†	0.4	5.1	46.0	36.3	†	†	†	†	102.3	
$^4D_{3/2}$	0.7	5.4	5.8	0.1	0.8	0.1	†	12.2	0.8	†	†	0.2	0.9	†	†	†	†	17.1	8.4	45.0	56.9	†	†	†	†	154.4	
$^4D_{5/2}$	1.7	5.4	10.3	0.2	1.8	0.5	†	8.6	0.8	†	†	0.3	1.4	†	†	†	0.2	†	40.5	18.3	58.8	87.5	†	†	†	†	236.3
$^4D_{7/2}$	2.7	12.2	19.0	0.3	3.0	0.8	0.3	13.7	0.8	†	†	0.7	1.0	†	†	†	0.4	0.1	64.1	35.0	150.3	153.1	†	†	†	†	457.5
$^2S_{1/2}$	0.2	0.1	†	†	0.1	†	†	0.4	†	†	†	0.1	†	†	†	†	†	0.1	0.2	0.8	4.8	†	†	†	†	6.8	
$^4S_{3/2}$	†	0.2	†	†	0.1	†	†	0.5	0.1	†	†	†	0.1	†	†	†	†	0.1	0.8	0.2	3.9	†	†	†	†	6.0	
$^2S_{1/2}$	0.3	0.1	1.7	†	†	6.6	0.1	0.1	†	0.5	0.2	0.2	0.2	1.0	4.0	†	3.5	0.1	†	†	†	†	†	†	†	18.6	
$^4S_{3/2}$	0.2	0.4	2.6	†	†	0.2	9.2	0.2	†	0.1	0.6	†	0.2	0.8	0.3	6.0	0.1	4.8	†	†	†	†	†	†	†	25.7	
$^2D_{3/2}$	7.7	94.8	†	0.9	†	37.7	0.4	166.5	17.1	†	†	3.0	36.8	1.6	†	†	18.0	0.2	†	†	†	†	1.7	0.1	†	†	386.5
$^2D_{5/2}$	77.0	78.6	†	9.3	†	3.8	6.1	84.8	4.2	0.3	†	20.6	5.5	2.4	†	†	1.9	2.9	†	†	†	†	20.6	15.6	†	†	333.6
$^2P_{1/2}$	†	1.7	†	†	†	0.2	†	1.6	0.2	†	†	†	0.3	†	†	†	0.1	†	†	†	†	†	3.2	0.7	†	†	8.0
$^2P_{3/2}$	1.0	0.9	†	0.1	†	0.1	†	1.7	0.1	†	†	0.3	0.2	†	†	†	†	†	†	†	†	†	24.3	3.5	†	†	32.2
$^2S_{1/2}$	8.6	4.4	†	0.4	†	23.7	4.9	7.5	1.9	†	†	3.5	9.4	3.7	†	†	11.9	2.3	†	†	†	†	16.7	0.9	†	†	99.8
$^2D_{3/2}$	43.6	4.5	84.1	4.2	9.9	159.7	0.4	3.1	2.0	3.3	2.9	8.4	7.7	12.4	46.8	†	81.8	0.2	†	†	†	†	†	†	0.8	0.1	475.9
$^2D_{5/2}$	80.7	46.1	126.5	10.2	23.4	200.6	1.1	68.6	4.5	9.7	0.8	23.6	7.9	2.3	14.2	0.2	96.6	0.6	†	†	†	†	†	†	2.8	1.7	722.1
$^4D_{1/2}$	14.5	16.2	137.8	0.8	8.1	10.3	564.6	14.2	4.4	0.4	4.8	0.6	14.0	17.0	3.0	43.9	5.2	284.8	†	†	†	†	†	†	†	5.5	1150.1
$^4D_{3/2}$	12.8	4.4	94.4	1.3	11.9	19.3	226.5	33.4	2.1	1.0	8.7	2.5	10.4	33.5	7.2	42.4	9.8	115.9	†	†	†	†	†	†	4.6	9.5	651.6
$^4D_{5/2}$	12.5	68.8	64.8	1.9	17.3	13.8	21.5	62.7	6.9	2.4	9.3	4.9	15.2	20.8	5.8	17.8	6.9	10.8	†	†	†	†	†	†	32.0	16.0	412.1
$^4D_{7/2}$	30.7	173.4	186.5	3.9	35.8	56.6	529.9	275.3	21.7	3.9	11.2	8.8	45.4	54.9	9.0	22.1	27.8	255.6	†	†	†	†	†	†	126.8	†	1879.3

TABLE X: Same as IX but for $\Sigma_c(nnc)$ resonances. The order of the states is the same as is presented in Table V. N_1^* , N_2^* , N_3^* , and N_4^* , represent $N(1520)$, $N(1535)$, $N(1680)$, and $N(1720)$ respectively.

State	$\Lambda_c K$	$\Xi_c \pi$	$\Xi'_c \pi$	$\Xi_c^* \pi$	$\Sigma_c K$	$\Sigma_c^* K$	$\Xi_c \eta$	$\Lambda_c K^* \Xi_c \rho$	$\Xi'_c \rho$	$\Xi_c^* \rho$	$\Sigma_c K^* \Sigma_c^* K^* \Xi'_c \eta$	$\Xi_c^* \eta$	$\Xi_c \eta'$	$\Xi'_c \eta'$	$\Xi_c^* \eta'$	$\Xi_c \omega$	$\Xi'_c \omega$	$\Xi_c^* \omega$	$\Xi_c \phi$	$\Xi'_c \phi$	$\Xi_c^* \phi$	$\Sigma_8 D$	$\Xi_8 D_8$	$\Sigma_8 D^* \Sigma_{10} D$	Tot	Γ
$^2S_{1/2}$	†	†	†	†	†	†	†	†	†	†	†	†	†	†	†	†	†	†	†	†	†	†	†	†	†	
$^4S_{3/2}$	†	0.4	†	†	†	†	†	†	†	†	†	†	†	†	†	†	†	†	†	†	†	†	†	†	0.4	
$^2P_{1/2}$	0.7	0.4	1.1	5.1	†	†	†	†	†	†	†	†	†	†	†	†	†	†	†	†	†	†	†	†	7.3	
$^4P_{1/2}$	0.8	0.4	0.5	3.2	0.2	†	†	†	†	†	†	†	†	†	†	†	†	†	†	†	†	†	†	†	5.1	
$^2P_{3/2}$	8.3	9.5	9.4	0.7	†	†	†	†	†	†	†	†	†	†	†	†	†	†	†	†	†	†	†	†	27.9	
$^4P_{3/2}$	1.8	2.1	0.5	13.9	0.6	†	†	†	†	†	†	†	†	†	†	†	†	†	†	†	†	†	†	†	18.9	
$^4P_{5/2}$	11.3	13.4	3.6	6.2	7.4	1.1	0.1	†	†	†	†	†	†	†	†	†	†	†	†	†	†	†	†	†	43.1	
$^2P_{1/2}$	†	†	0.4	52.2	5.5	98.5	†	†	†	†	†	†	†	†	†	†	†	†	†	†	†	†	†	†	156.6	
$^2P_{3/2}$	†	†	21.7	11.9	50.4	15.9	†	†	†	†	†	†	†	†	†	†	†	†	†	†	†	†	†	†	99.9	
$^2D_{3/2}$	0.6	0.7	0.7	1.1	1.6	2.2	0.1	0.4	†	†	†	†	†	†	†	†	†	†	†	†	†	†	†	†	20.5	
$^2D_{5/2}$	1.8	2.2	2.2	0.3	4.6	0.6	0.2	0.1	†	†	†	†	†	0.1	†	†	†	†	†	†	†	†	†	†	64.5	
$^4D_{1/2}$	†	†	†	1.6	0.1	3.3	†	0.6	0.1	†	†	†	†	†	†	†	†	†	†	†	†	†	†	†	28.9	
$^4D_{3/2}$	0.7	0.8	0.2	2.1	0.5	4.6	0.1	1.8	0.4	†	†	†	†	†	0.1	†	†	†	†	†	†	†	†	†	53.0	
$^4D_{5/2}$	1.6	2.0	0.5	1.9	1.1	4.3	0.2	1.7	1.1	†	†	†	†	†	0.1	†	†	†	†	†	†	†	†	†	97.2	
$^4D_{7/2}$	2.5	3.1	0.8	2.7	1.7	5.2	0.3	2.0	1.3	†	†	0.1	†	0.1	0.1	†	†	†	†	†	†	†	†	†	160.5	
$^2S_{1/2}$	†	0.1	0.1	†	0.2	0.1	†	0.1	†	†	†	†	†	†	†	†	†	†	†	†	†	†	†	†	2.4	
$^4S_{3/2}$	†	†	†	0.1	0.1	0.3	†	0.1	0.1	†	†	†	†	†	†	†	†	†	†	†	†	†	†	†	4.4	
$^2S_{1/2}$	†	†	0.1	0.1	0.2	0.2	†	0.4	0.8	5.0	0.1	10.9	0.1	†	†	0.4	†	†	0.3	1.7	†	0.3	†	†	20.6	
$^4S_{3/2}$	0.1	†	†	0.1	†	0.2	†	0.2	0.6	0.3	7.3	0.6	15.9	†	0.1	0.4	0.1	0.1	0.2	0.1	2.4	0.6	†	†	29.3	
$^2D_{3/2}$	†	†	1.7	40.4	4.0	90.1	†	39.1	34.0	1.2	†	4.0	†	0.3	2.8	†	†	†	10.7	0.3	†	†	†	†	228.6	
$^2D_{5/2}$	†	†	22.7	11.8	48.4	22.3	†	11.3	9.1	0.8	†	2.1	0.2	1.7	0.3	†	†	†	2.9	0.2	†	†	†	†	133.8	
$^2P_{1/2}$	†	†	†	0.6	†	1.2	†	0.3	0.2	†	†	†	†	†	†	†	†	†	0.1	†	†	†	†	†	2.4	
$^2P_{3/2}$	†	†	0.4	0.3	0.8	0.7	†	0.4	0.3	†	†	†	†	†	†	†	†	†	0.1	†	†	†	†	†	3.0	
$^2S_{1/2}$	†	†	0.3	2.5	1.4	8.4	†	9.7	15.1	3.1	†	8.6	†	0.5	1.0	†	†	†	5.0	0.8	†	†	†	†	56.4	
$^2D_{3/2}$	8.4	9.4	8.1	4.5	17.2	10.6	0.6	4.2	8.9	66.7	†	151.6	0.1	0.6	0.8	1.8	†	†	3.0	21.8	†	1.4	†	†	319.7	
$^2D_{5/2}$	16.8	20.4	21.0	8.8	45.3	18.7	1.7	6.2	3.4	20.1	0.4	51.4	1.0	1.8	0.4	5.7	1.2	†	1.1	6.4	0.1	0.3	†	†	232.2	
$^4D_{1/2}$	10.4	9.7	1.2	10.0	2.3	22.6	0.2	8.5	13.8	3.9	139.6	8.8	345.6	†	1.3	1.4	0.1	†	4.6	1.3	43.9	2.6	†	†	631.8	
$^4D_{3/2}$	10.1	11.3	2.5	5.4	5.2	12.6	0.7	16.0	26.3	8.0	85.1	17.8	200.3	0.2	1.2	2.5	0.1	†	8.8	2.6	27.4	8.1	†	†	452.2	
$^4D_{5/2}$	10.9	14.3	4.1	13.5	9.0	29.3	1.4	11.9	16.2	5.2	16.9	11.2	34.4	0.4	1.2	5.8	0.6	0.4	5.4	1.7	5.7	8.2	0.2	†	207.9	
$^4D_{7/2}$	25.7	31.2	7.9	43.1	17.1	93.8	2.6	51.1	51.9	9.9	40.0	24.5	117.6	0.6	2.9	10.5	2.1	1.5	16.9	3.2	12.4	10.7	0.8	0.2	†	578.2

TABLE XI: Same as IX but for $\Xi'_c(snc)$ resonances. The order of the states is the same as is presented in Table VI.

State	$\Lambda_c K$	$\Xi_c \pi$	$\Xi'_c \pi$	$\Xi_c^* \pi$	$\Sigma_c K$	$\Sigma_c^* K$	$\Xi_c \eta$	$\Lambda_c K^* \Xi_c \rho$	$\Xi'_c \rho$	$\Xi_c^* \rho$	$\Sigma_c K^* \Sigma_c^* K^* \Xi'_c \eta$	$\Xi_c^* \eta$	$\Xi_c \eta'$	$\Xi'_c \eta'$	$\Xi_c^* \eta'$	$\Xi_c \omega$	$\Xi'_c \omega$	$\Xi_c^* \omega$	$\Xi_c \phi$	$\Xi'_c \phi$	$\Xi_c^* \phi$	$\Lambda_8 D$	$\Lambda_8 D^*$	$\Sigma_8 D$	$\Lambda_8^* D$	Tot Γ
$^2S_{1/2}$	†	†	†	†	†	†	†	†	†	†	†	†	†	†	†	†	†	†	†	†	†	†	†	†	†	†
$^2P_{1/2}$	†	†	0.6	2.0	†	†	†	†	†	†	†	†	†	†	†	†	†	†	†	†	†	†	†	†	†	2.6
$^2P_{3/2}$	†	†	3.9	0.6	†	†	†	†	†	†	†	†	†	†	†	†	†	†	†	†	†	†	†	†	†	4.5
$^2P_{1/2}$	0.8	0.4	2.0	13.3	0.5	†	†	†	†	†	†	†	†	†	†	†	†	†	†	†	†	†	†	†	†	17.0
$^4P_{1/2}$	0.6	0.2	0.7	7.7	3.4	0.3	†	†	†	†	†	†	†	†	†	†	†	†	†	†	†	†	†	†	†	12.9
$^2P_{3/2}$	18.7	21.8	22.7	2.0	23.9	†	†	†	†	†	†	†	†	†	†	†	†	†	†	†	†	†	†	†	†	89.1
$^4P_{3/2}$	4.0	4.7	1.3	31.5	2.5	12.2	†	†	†	†	†	†	†	†	†	†	†	†	†	†	†	†	†	†	†	56.2
$^4P_{5/2}$	25.5	30.8	8.4	17.0	19.2	19.0	2.2	†	†	†	†	†	†	†	†	†	†	†	†	†	†	†	†	†	†	122.1
$^2D_{3/2}$	†	†	0.4	2.2	0.8	2.9	†	†	†	†	†	†	†	†	†	†	†	†	†	†	†	†	†	†	†	50.5
$^2D_{5/2}$	†	†	1.2	0.5	2.2	0.6	†	†	†	†	†	†	†	†	†	†	†	†	†	†	†	†	†	†	†	131.8
$^2S_{1/2}$	†	†	0.1	0.1	0.1	0.2	†	†	†	†	†	†	†	†	†	†	†	†	†	†	†	†	†	†	†	5.2
$^2S_{1/2}$	†	†	0.2	0.5	0.4	1.2	†	0.9	1.3	0.5	†	1.1	0.1	†	0.1	†	†	†	†	†	†	†	†	†	†	6.8
$^2D_{3/2}$	1.3	1.7	2.5	10.6	6.3	21.8	0.3	6.9	1.6	†	†	†	†	†	†	†	†	†	†	†	†	†	†	†	†	53.9
$^2D_{5/2}$	18.3	22.3	22.1	1.8	46.0	3.1	1.6	1.1	0.8	†	†	†	†	†	†	†	†	†	†	†	†	†	†	†	†	118.6
$^4D_{1/2}$	0.2	0.4	0.5	4.6	1.7	9.8	0.4	3.7	1.5	†	†	†	†	†	†	†	†	†	†	†	†	†	†	†	†	23.5
$^4D_{3/2}$	1.4	1.7	0.6	17.4	1.5	39.0	0.3	16.8	9.5	†	†	†	†	†	†	†	†	†	†	†	†	†	†	†	†	91.9
$^4D_{5/2}$	8.1	9.8	2.5	23.8	5.2	52.7	0.7	23.0	18.4	0.2	†	0.8	†	0.2	1.5	†	†	†	†	†	†	†	†	†	†	152.6
$^4D_{7/2}$	30.6	37.1	9.4	20.1	20.1	39.4	3.0	15.4	10.2	0.6	0.3	1.8	1.0	0.7	0.7	0.3	†	†	†	†	†	†	†	†	†	194.2
$^2P_{1/2}$	†	†	†	0.1	†	0.2	†	†	†	†	†	†	†	†	†	†	†	†	†	†	†	†	†	†	†	0.3
$^2P_{3/2}$	0.3	0.4	0.4	0.1	0.7	0.1	†	†	†	†	†	†	†	†	†	†	†	†	†	†	†	†	†	†	†	2.0
$^4P_{1/2}$	†	†	†	0.1	†	0.1	†	†	†	†	†	†	†	†	†	†	†	†	†	†	†	†	†	†	†	0.2
$^4P_{3/2}$	0.1	0.1	†	0.3	†	0.5	†	0.2	0.1	†	†	†	†	†	†	†	†	†	†	†	†	†	†	†	†	1.3
$^4P_{5/2}$	0.5	0.6	0.1	0.4	0.3	0.9	†	0.4	0.3	†	†	†	†	†	†	†	†	†	†	†	†	†	†	†	†	3.6
$^4S_{3/2}$	0.9	0.3	0.3	3.1	1.0	9.7	0.3	7.2	8.7	0.2	†	0.8	†	0.2	0.7	†	†	†	†	†	†	†	†	†	†	36.3
$^2S_{1/2}$	0.1	0.3	2.5	1.9	8.0	5.3	0.4	6.2	3.4	†	†	†	†	†	†	†	†	†	†	†	†	†	†	†	†	29.8
$^2D_{3/2}$	†	†	4.1	16.4	8.7	38.9	†	19.5	23.1	3.3	†	8.7	†	0.3	1.9	†	†	†	†	†	†	†	†	†	†	133.3
$^2D_{5/2}$	†	†	12.0	15.2	25.7	30.5	†	14.7	12.2	0.4	0.3	0.8	1.0	0.5	†	†	†	†	†	†	†	†	†	†	†	118.4

TABLE XII: Same as IX but for $\Xi_c(snc)$ resonances. The order of the states is the same as is presented in Table VI.

State	$\Sigma_c\pi$	$\Sigma_c^*\pi$	$\Lambda_c\eta$	$\Sigma_c\rho$	$\Sigma^*\rho$	$\Lambda_c\eta'$	$\Lambda_c\omega$	Ξ_cK	Ξ'_cK	Ξ_c^*K	Ξ_cK^*	Ξ'_cK^*	$\Xi_c^*K^*$	ND	Tot Γ
$^2S_{1/2}$	†	†	†	†	†	†	†	†	†	†	†	†	†	†	†
$^2P_{1/2}$	1.4	†	†	†	†	†	†	†	†	†	†	†	†	†	1.4
$^2P_{3/2}$	9.7	0.1	†	†	†	†	†	†	†	†	†	†	†	†	9.8
$^2P_{1/2}$	7.3	49.6	†	†	†	†	†	†	†	†	†	†	†	†	56.9
$^4P_{1/2}$	2.6	28.5	1.4	†	†	†	†	†	†	†	†	†	†	†	32.5
$^2P_{3/2}$	83.9	7.7	1.1	†	†	†	†	†	†	†	†	†	†	†	92.7
$^4P_{3/2}$	4.7	115.8	1.4	†	†	†	†	†	†	†	†	†	†	†	121.9
$^4P_{5/2}$	31.2	64.6	12.2	†	†	†	†	0.1	†	†	†	†	†	†	108.1
$^2D_{3/2}$	1.7	8.8	†	†	†	†	†	†	†	†	†	†	†	59.1	69.6
$^2D_{5/2}$	4.7	2.0	†	†	†	†	†	†	†	†	†	†	†	164.5	171.2
$^2S_{1/2}$	0.2	0.4	†	†	†	†	†	†	†	†	†	†	†	4.7	5.3
$^2S_{1/2}$	0.2	0.7	†	2.5	0.4	†	1.1	†	0.4	0.8	0.2	†	†	†	6.3
$^2D_{3/2}$	9.0	42.0	1.0	†	†	†	13.3	2.7	1.6	0.7	†	†	†	†	70.3
$^2D_{5/2}$	90.0	10.1	8.3	0.4	†	†	1.7	13.9	8.4	0.2	†	†	†	†	133.0
$^4D_{1/2}$	1.0	19.9	0.6	†	†	†	7.5	3.8	0.8	0.7	†	†	†	†	34.3
$^4D_{3/2}$	2.2	63.0	0.9	0.4	†	†	31.5	2.9	0.6	4.5	†	†	†	†	106.0
$^4D_{5/2}$	10.3	86.6	3.8	3.9	0.1	0.2	39.9	6.7	1.2	10.0	†	†	†	†	162.7
$^4D_{7/2}$	37.3	99.2	13.9	4.5	2.8	5.7	29.8	26.8	5.7	4.4	†	†	†	†	230.1
$^2P_{1/2}$	†	0.4	†	†	†	†	0.1	†	†	†	†	†	†	†	0.5
$^2P_{3/2}$	1.2	0.3	0.1	†	†	†	†	0.2	0.1	†	†	†	†	†	1.9
$^4P_{1/2}$	†	0.3	†	†	†	†	†	†	†	†	†	†	†	†	0.3
$^4P_{3/2}$	0.1	0.9	†	†	†	†	0.3	†	†	†	†	†	†	†	1.3
$^4P_{5/2}$	0.5	1.4	0.2	0.1	†	†	0.6	0.3	0.1	0.1	†	†	†	†	3.3
$^4S_{3/2}$	0.3	4.7	0.2	2.9	1.2	0.7	11.2	3.9	1.6	5.6	†	†	†	†	32.3
$^2S_{1/2}$	4.1	4.4	0.7	0.1	†	†	10.8	4.8	4.4	0.8	†	†	†	†	30.1
$^2D_{3/2}$	21.0	49.6	†	26.4	0.3	†	33.3	†	3.5	18.8	0.7	†	†	†	153.6
$^2D_{5/2}$	54.3	90.1	†	2.1	3.8	†	34.5	†	10.0	5.4	1.5	†	†	†	201.7

TABLE XIII: Same as IX but for $\Lambda_c(nnc)$ resonances. The order of the states is the same as is presented in Table VIII.

Appendix G: Decay products

Here we give the masses of the final baryons and mesons states used in our calculation of the decay widths.

	Mass in GeV
m_π	0.13725 ± 0.00295
m_K	0.49564 ± 0.00279
m_η	0.54786 ± 0.00002
$m_{\eta'}$	0.95778 ± 0.00006
m_ρ	0.77518 ± 0.00045
m_{K^*}	0.89555 ± 0.00100
m_ω	0.78266 ± 0.00002
m_ϕ	1.01946 ± 0.00002
m_D	1.86672 ± 0.00193
m_{D_s}	1.96835 ± 0.00007
m_{D^*}	2.00855 ± 0.00180
m_N	0.93891 ± 0.00091
$m_{N(1520)}$	1.51500 ± 0.00500
$m_{N(1535)}$	1.53000 ± 0.01500
$m_{N(1680)}$	1.68500 ± 0.00500
$m_{N(1720)}$	1.72000 ± 0.03500
m_Δ	1.23200 ± 0.00200
m_Λ	1.11568 ± 0.00001
$m_{\Lambda(1520)}$	1.51900 ± 0.00010
m_{Ξ_8}	1.31820 ± 0.00360
$m_{\Xi_{10}}$	1.53370 ± 0.00250
m_{Σ_8}	1.11932 ± 0.00340
$m_{\Sigma_{10}}$	1.38460 ± 0.00460
m_{Λ_c}	2.28646 ± 0.00014
m_{Ξ_c}	2.46908 ± 0.00158
$m_{\Xi'_c}$	2.57850 ± 0.00100
$m_{\Xi_c^*}$	2.64563 ± 0.00100
m_{Σ_c}	2.45350 ± 0.00090
$m_{\Sigma_c^*}$	2.51813 ± 0.00280
m_{Ω_c}	2.69520 ± 0.00170
$m_{\Omega_c^*}$	2.76590 ± 0.00200

TABLE XIV: Masses of final baryon and meson used in the calculation of decay width. The masses were taken from Ref. [9].

-
- [1] R. Aaij, *et al.*, Phys. Rev. Lett. **118**, 182001 (2017). DOI 10.1103/PhysRevLett.118.182001. URL <https://link.aps.org/doi/10.1103/PhysRevLett.118.182001>
- [2] J. Yelton *et al.* [Belle collaboration], Phys. Rev. D **97**, 051102 (2018). DOI 10.1103/PhysRevD.97.051102. URL <https://link.aps.org/doi/10.1103/PhysRevD.97.051102>
- [3] R. Aaij, *et al.*, Phys. Rev. Lett. **124**(22), 222001 (2020). DOI 10.1103/PhysRevLett.124.222001
- [4] Y.B. Li, *et al.*, Eur. Phys. J. C **78**(3), 252 (2018). DOI 10.1140/epjc/s10052-018-5720-5
- [5] B. Aubert, *et al.*, Phys. Rev. D **77**, 031101 (2008). DOI 10.1103/PhysRevD.77.031101
- [6] J. Yelton, *et al.*, Phys. Rev. D **94**(5), 052011 (2016). DOI 10.1103/PhysRevD.94.052011
- [7] R. Chistov, *et al.*, Phys. Rev. Lett. **97**, 162001 (2006). DOI 10.1103/PhysRevLett.97.162001
- [8] B. Aubert, *et al.*, Phys. Rev. D **77**, 012002 (2008). DOI 10.1103/PhysRevD.77.012002
- [9] P. Zyla, *et al.*, PTEP **2020**(8), 083C01 (2020). DOI 10.1093/ptep/ptaa104
- [10] J. Yelton, *et al.*, Phys. Rev. D **104**(5), 052003 (2021). DOI 10.1103/PhysRevD.104.052003
- [11] T. J. Moon *et al.* [Belle collaboration], Phys. Rev. D **103**, L111101 (2021). DOI 10.1103/PhysRevD.103.L111101. URL <https://link.aps.org/doi/10.1103/PhysRevD.103.L111101>
- [12] N. Isgur, G. Karl, Physics Letters B **72**(1), 109 (1977). DOI [https://doi.org/10.1016/0370-2693\(77\)90074-0](https://doi.org/10.1016/0370-2693(77)90074-0). URL <https://www.sciencedirect.com/science/article/pii/0370269377900740>
- [13] N. Isgur, G. Karl, Phys. Rev. D **18**, 4187 (1978). DOI 10.1103/PhysRevD.18.4187
- [14] L.A. Copley, N. Isgur, G. Karl, Phys. Rev. D **20**, 768 (1979). DOI 10.1103/PhysRevD.20.768. [Erratum: Phys.Rev.D 23, 817 (1981)]
- [15] S. Capstick, N. Isgur, AIP Conf. Proc. **132**, 267 (1985). DOI 10.1103/PhysRevD.34.2809
- [16] D. Ebert, R.N. Faustov, V.O. Galkin, Phys. Rev. D **84**, 014025 (2011). DOI 10.1103/PhysRevD.84.014025
- [17] D. Ebert, R.N. Faustov, V.O. Galkin, Phys. Lett. B **659**, 612 (2008). DOI 10.1016/j.physletb.2007.11.037
- [18] W. Roberts, M. Pervin, Int. J. Mod. Phys. A **23**, 2817 (2008). DOI 10.1142/S0217751X08041219
- [19] T. Yoshida, E. Hiyama, A. Hosaka, M. Oka, K. Sadato, Phys. Rev. D **92**(11), 114029 (2015). DOI 10.1103/PhysRevD.92.114029
- [20] B. Chen, K.W. Wei, X. Liu, T. Matsuki, Eur. Phys. J. C **77**(3), 154 (2017). DOI 10.1140/epjc/s10052-017-4708-x
- [21] H.X. Chen, W. Chen, Q. Mao, A. Hosaka, X. Liu, S.L. Zhu, Phys. Rev. D **91**(5), 054034 (2015). DOI 10.1103/PhysRevD.91.054034
- [22] H.X. Chen, Q. Mao, A. Hosaka, X. Liu, S.L. Zhu, Phys. Rev. D **94**(11), 114016 (2016). DOI 10.1103/PhysRevD.94.114016
- [23] E. Bagan, M. Chabab, H.G. Dosch, S. Narison, Phys. Lett. B **287**, 176 (1992). DOI 10.1016/0370-2693(92)91896-H
- [24] H.M. Yang, H.X. Chen, Phys. Rev. D **104**(3), 034037 (2021). DOI 10.1103/PhysRevD.104.034037
- [25] H. Garcilazo, J. Vijande, A. Valcarce, J. Phys. G **34**, 961 (2007). DOI 10.1088/0954-3899/34/5/014
- [26] P. Hasenfratz, R.R. Horgan, J. Kuti, J.M. Richard, Phys. Lett. B **94**, 401 (1980). DOI 10.1016/0370-2693(80)90906-5
- [27] M.J. Savage, Phys. Lett. B **359**, 189 (1995). DOI 10.1016/0370-2693(95)01060-4
- [28] Y. Kim, E. Hiyama, M. Oka, K. Suzuki, Phys. Rev. D **102**(1), 014004 (2020). DOI 10.1103/PhysRevD.102.014004
- [29] Y. Kim, Y.R. Liu, M. Oka, K. Suzuki, Phys. Rev. D **104**(5), 054012 (2021). DOI 10.1103/PhysRevD.104.054012
- [30] J. Vijande, A. Valcarce, H. Garcilazo, Phys. Rev. D **90**(9), 094004 (2014). DOI 10.1103/PhysRevD.90.094004
- [31] L. Liu, H.W. Lin, K. Orginos, A. Walker-Loud, Phys. Rev. D **81**, 094505 (2010). DOI 10.1103/PhysRevD.81.094505
- [32] R.A. Briceño, H.W. Lin, D.R. Bolton, Phys. Rev. D **86**, 094504 (2012). DOI 10.1103/PhysRevD.86.094504
- [33] H. Bahtiyar, K.U. Can, G. Erkol, P. Gubler, M. Oka, T.T. Takahashi, Phys. Rev. D **102**(5), 054513 (2020). DOI 10.1103/PhysRevD.102.054513
- [34] J.G. Körner, M. Kramer, D. Pirjol, Prog. Part. Nucl. Phys. **33**, 787 (1994). DOI 10.1016/0146-6410(94)90053-1
- [35] H.X. Chen, W. Chen, X. Liu, Y.R. Liu, S.L. Zhu, Rept. Prog. Phys. **80**(7), 076201 (2017). DOI 10.1088/1361-6633/aa6420
- [36] V. Crede, W. Roberts, Rept. Prog. Phys. **76**, 076301 (2013). DOI 10.1088/0034-4885/76/7/076301
- [37] Y.S. Amhis, *et al.*, Eur. Phys. J. C **81**(3), 226 (2021). DOI 10.1140/epjc/s10052-020-8156-7
- [38] H.Y. Cheng, Front. Phys. (Beijing) **10**(6), 101406 (2015). DOI 10.1007/s11467-015-0483-z
- [39] X.H. Zhong, Q. Zhao, Phys. Rev. D **77**, 074008 (2008). DOI 10.1103/PhysRevD.77.074008
- [40] L.H. Liu, L.Y. Xiao, X.H. Zhong, Phys. Rev. D **86**, 034024 (2012). DOI 10.1103/PhysRevD.86.034024
- [41] K.L. Wang, Y.X. Yao, X.H. Zhong, Q. Zhao, Phys. Rev. D **96**(11), 116016 (2017). DOI 10.1103/PhysRevD.96.116016
- [42] H.Y. Cheng, C.K. Chua, Phys. Rev. D **75**, 014006 (2007). DOI 10.1103/PhysRevD.75.014006
- [43] H.Y. Cheng, C.K. Chua, Phys. Rev. D **92**(7), 074014 (2015). DOI 10.1103/PhysRevD.92.074014
- [44] H. Nagahiro, S. Yasui, A. Hosaka, M. Oka, H. Noumi, Phys. Rev. D **95**(1), 014023 (2017). DOI 10.1103/PhysRevD.95.014023
- [45] A.J. Arifi, D. Suenaga, A. Hosaka, Phys. Rev. D **103**(9), 094003 (2021). DOI 10.1103/PhysRevD.103.094003
- [46] Y.X. Yao, K.L. Wang, X.H. Zhong, Phys. Rev. D **98**(7), 076015 (2018). DOI 10.1103/PhysRevD.98.076015
- [47] S.L. Zhu, Phys. Rev. D **61**, 114019 (2000). DOI 10.1103/PhysRevD.61.114019
- [48] H.X. Chen, Q. Mao, W. Chen, A. Hosaka, X. Liu, S.L. Zhu, Phys. Rev. D **95**(9), 094008 (2017). DOI 10.1103/PhysRevD.95.094008
- [49] C. Chen, X.L. Chen, X. Liu, W.Z. Deng, S.L. Zhu, Phys. Rev. D **75**, 094017 (2007). DOI 10.1103/PhysRevD.75.094017. URL <https://link.aps.org/doi/10.1103/PhysRevD.75.094017>
- [50] J.J. Guo, P. Yang, A. Zhang, Phys. Rev. D **100**(1), 014001 (2019). DOI 10.1103/PhysRevD.100.014001

- [51] K. Gong, H.Y. Jing, A. Zhang, Eur. Phys. J. C **81**(5), 467 (2021). DOI 10.1140/epjc/s10052-021-09255-w
- [52] Q.F. Lü, L.Y. Xiao, Z.Y. Wang, X.H. Zhong, Eur. Phys. J. C **78**(7), 599 (2018). DOI 10.1140/epjc/s10052-018-6083-7
- [53] E. Santopinto, A. Giachino, J. Ferretti, H. García-Tecocoatzi, M.A. Bedolla, R. Bijker, E. Ortiz-Pacheco, The European Physical Journal C **79**(12), 1012 (2019). DOI 10.1140/epjc/s10052-019-7527-4. URL <https://doi.org/10.1140/epjc/s10052-019-7527-4>
- [54] R. Bijker, H. García-Tecocoatzi, A. Giachino, E. Ortiz-Pacheco, E. Santopinto, Phys. Rev. D **105**(7), 074029 (2022). DOI 10.1103/PhysRevD.105.074029
- [55] B. Efron, R.J. Tibshirani, *An introduction to the bootstrap*. Mono. Stat. Appl. Probab. (Chapman and Hall, London, 1993). URL <https://cds.cern.ch/record/526679>
- [56] S. Capstick, W. Roberts, Phys. Rev. D **47**, 1994 (1993). DOI 10.1103/PhysRevD.47.1994. URL <https://link.aps.org/doi/10.1103/PhysRevD.47.1994>
- [57] N. Isgur, G. Karl, Phys. Rev. D **18**, 4187 (1978). DOI 10.1103/PhysRevD.18.4187. URL <https://link.aps.org/doi/10.1103/PhysRevD.18.4187>
- [58] L. Micu, Nuclear Physics B **10**(3), 521 (1969). DOI [https://doi.org/10.1016/0550-3213\(69\)90039-X](https://doi.org/10.1016/0550-3213(69)90039-X). URL <http://www.sciencedirect.com/science/article/pii/055032136990039X>
- [59] A. Le Yaouanc, L. Oliver, O. Pène, J.C. Raynal, Phys. Rev. D **8**, 2223 (1973). DOI 10.1103/PhysRevD.8.2223. URL <https://link.aps.org/doi/10.1103/PhysRevD.8.2223>
- [60] R. Bijker, J. Ferretti, G. Galatà, H. García-Tecocoatzi, E. Santopinto, Phys. Rev. D **94**, 074040 (2016). DOI 10.1103/PhysRevD.94.074040. URL <https://link.aps.org/doi/10.1103/PhysRevD.94.074040>
- [61] S. Godfrey, N. Isgur, Phys. Rev. D **32**, 189 (1985). DOI 10.1103/PhysRevD.32.189. URL <https://link.aps.org/doi/10.1103/PhysRevD.32.189>
- [62] R. Kokoski, N. Isgur, Phys. Rev. D **35**, 907 (1987). DOI 10.1103/PhysRevD.35.907. URL <https://link.aps.org/doi/10.1103/PhysRevD.35.907>
- [63] F.E. Close, E.S. Swanson, Phys. Rev. D **72**, 094004 (2005). DOI 10.1103/PhysRevD.72.094004. URL <https://link.aps.org/doi/10.1103/PhysRevD.72.094004>
- [64] H.G. Blundell, S. Godfrey, Phys. Rev. D **53**, 3700 (1996). DOI 10.1103/PhysRevD.53.3700. URL <https://link.aps.org/doi/10.1103/PhysRevD.53.3700>
- [65] D. Molina, M. De Sanctis, C. Fernández-Ramírez, E. Santopinto, The European Physical Journal C **80**(6), 526 (2020). DOI 10.1140/epjc/s10052-020-8099-z. URL <https://doi.org/10.1140/epjc/s10052-020-8099-z>
- [66] F. James, M. Roos, Computer Physics Communications **10**(6), 343 (1975). DOI [https://doi.org/10.1016/0010-4655\(75\)90039-9](https://doi.org/10.1016/0010-4655(75)90039-9). URL <http://www.sciencedirect.com/science/article/pii/0010465575900399>
- [67] C.R. Harris, K.J. Millman, S.J. van der Walt, R. Gommers, P. Virtanen, D. Cournapeau, E. Wieser, J. Taylor, S. Berg, N.J. Smith, R. Kern, M. Picus, S. Hoyer, M.H. van Kerkwijk, M. Brett, A. Haldane, J.F. del Río, M. Wiebe, P. Peterson, P. Gérard-Marchant, K. Sheppard, T. Reddy, W. Weckesser, H. Abbasi, C. Gohlke, T.E. Oliphant, Nature **585**(7825), 357 (2020). DOI 10.1038/s41586-020-2649-2. URL <https://doi.org/10.1038/s41586-020-2649-2>
- [68] M.a. Tanabashi, Phys. Rev. D **98**, 030001 (2018). DOI 10.1103/PhysRevD.98.030001. URL <https://link.aps.org/doi/10.1103/PhysRevD.98.030001>
- [69] J.J. de Swart, Rev. Mod. Phys. **35**, 916 (1963). DOI 10.1103/RevModPhys.35.916. [Erratum: Rev.Mod.Phys. 37, 326–326 (1965)]